

**Tuning Monte Carlo generators: The Perugia tunes**

Peter Z. Skands\*

*CERN PH-TH, Case 01600, CH-1211 Geneva 23, Switzerland*

(Received 28 June 2010; published 20 October 2010)

We present 9 new tunes of the  $p_{\perp}$ -ordered shower and underlying-event model in PYTHIA 6.4. These “Perugia” tunes update and supersede the older “S0” family. The data sets used to constrain the models include hadronic  $Z^0$  decays at LEP, Tevatron min-bias data at 630, 1800, and 1960 GeV, Tevatron Drell-Yan data at 1800 and 1960 GeV, and SPS min-bias data at 200, 546, and 900 GeV. In addition to the central parameter set, called “Perugia 0,” we introduce a set of 8 related “Perugia variations” that attempt to systematically explore soft, hard, parton density, and color structure variations in the theoretical parameters. Based on these variations, a best-guess prediction of the charged track multiplicity in inelastic, nondiffractive minimum-bias events at the LHC is made. Note that these tunes can only be used with PYTHIA 6, not with PYTHIA 8.

DOI: 10.1103/PhysRevD.82.074018

PACS numbers: 12.38.Lg, 12.38.Cy, 13.85.Hd, 13.87.Fh

**I. INTRODUCTION**

Perturbative calculations of collider observables rely on two important prerequisites: factorization and infrared (IR) safety. These are the tools that permit us to relate theoretical calculations to detector-level measured quantities, up to corrections of known dimensionality, which can then be suppressed (or enhanced) by appropriate choices of the dimensionful scales appearing in the observable and process under study. However, in the context of the underlying event (UE), say, we are faced with the fact that we do not (yet) have formal factorization theorems for this component—in fact the most naive attempts at factorization can easily be shown to fail [1,2]. At the same time, not all collider measurements can be made insensitive to the UE at a level comparable to the achievable experimental precision, and hence the extraction of parameters from such measurements acquires an implicit dependence on our modeling of the UE. Further, when considering observables such as track multiplicities, hadronization corrections, or even short-distance quantities if the precision required is very high, we are confronted with observables which may be experimentally well measured, but which are explicitly sensitive to infrared physics.

(a) *The role of factorization:* Let us begin with factorization. When applicable, factorization allows us to subdivide the calculation of an observable (regardless of whether it is IR safe or not) into a perturbatively calculable short-distance part and an approximately universal long-distance part, the latter of which may be modeled and constrained by fits to data. However, in the context of hadron collisions, the possibilities of multiple perturbative parton-parton interactions and parton rescattering processes explicitly go beyond the factorization theorems so far developed. Part of the problem is that the underlying event may contain short-distance physics of its own that

can be as hard as, or even harder than, the bremsstrahlung emissions associated with the scattering that triggered the event. Hence the conceptual separation into what we think of as “hard-scattering” and “underlying-event” components is not necessarily equivalent to a clean separation in terms of “short-distance” and “long-distance” physics. Indeed, from ISR energies [3] through the SPS [4,5] to the Tevatron [6–10], and also in photoproduction at HERA [11], we see evidence of (perturbative) “minijets” in the underlying event, beyond what bremsstrahlung alone appears to be able to account for. It therefore appears plausible that a universal modeling of the underlying event must take into account that the hard-scattering and underlying-event components can involve similar time scales and have a common, correlated evolution. It is in this spirit that the concept of “interleaved evolution” [12] was developed as the cornerstone of the  $p_{\perp}$ -ordered models [12,13] in both PYTHIA 6 [14] and, more recently, PYTHIA 8 [15], the latter of which now also incorporates a model of parton rescattering [16].

(b) *The role of infrared safety:* The second tool, infrared safety,<sup>1</sup> provides us with a class of observables which are insensitive to the details of the long-distance physics. This works up to corrections of order the long-distance scale divided by the short-distance scale to some (observable-dependent) power, typically

$$\text{IR safe corrections} \propto \frac{Q_{\text{IR}}^2}{Q_{\text{UV}}^2}, \quad (1)$$

where  $Q_{\text{UV}}$  denotes a generic hard scale in the problem, and  $Q_{\text{IR}} \sim \Lambda_{\text{QCD}} \sim \mathcal{O}(1 \text{ GeV})$ . Of course, in minimum bias, we typically have  $Q_{\text{UV}}^2 \sim Q_{\text{IR}}^2$ , wherefore *all* observables depend significantly on the IR physics (or in other

\*peter.skands@cern.ch

<sup>1</sup>By “infrared” we here mean any non-UV limit, without regard to whether it is collinear or soft.

words, when IR physics is all there is, then any observable, no matter how carefully defined, depends on it).

Even when a high scale is present, as in resonance decays, jet fragmentation, or underlying-event-type studies, infrared safety only guarantees us that infrared corrections are small, not that they are zero. Thus, ultimately, we run into a precision barrier even for IR safe observables, which only a reliable understanding of the long-distance physics itself can address.

Finally, there are the non-infrared-safe observables. Instead of the suppressed corrections above, such observables contain logarithms

$$\text{IR sensitive corrections} \propto \alpha_s^n \log^m \left( \frac{Q_{UV}^2}{Q_{IR}^2} \right), \quad m \leq 2n, \quad (2)$$

which grow increasingly large as  $Q_{IR}/Q_{UV} \rightarrow 0$ . As an example, consider such a fundamental quantity as particle multiplicities; in the absence of nontrivial infrared effects, the number of partons that would be mapped to hadrons in a naive local-parton-hadron-duality [17] picture would tend logarithmically to infinity as the IR cutoff is lowered. Similarly, the distinction between a charged and a neutral pion only occurs in the very last phase of hadronization, and hence observables that only include charged tracks are always IR sensitive.

(c) *Minimum bias and the underlying event:* Minimum-bias (MB) and UE physics can therefore be perceived of as offering an ideal lab for *studying* nonfactorized and non-perturbative phenomena, with the added benefit of having access to the highest possible statistics in the case of min-bias. In this context there is no strong preference for IR safe over IR sensitive observables; they merely represent two different lenses through which we can view the infrared physics, each revealing different aspects. By far the most important point is that it is in their *combination* that we achieve a sort of stereo vision, in which infrared safe observables measuring the overall energy flow are simply the slightly averaged progenitors of the spectra and correlations that appear at the level of individual particles. A systematic program of such studies can give crucial tests of our ability to model and understand these ubiquitous components, and the resulting improved physics models can then be fed back into the modeling of high- $p_{\perp}$  physics.

Starting from early notions such as “KNO scaling” of multiplicity distributions [18], a large number of theoretical and experimental investigations have been brought to bear on what the physics of a generic, unbiased sample of hadron collisions looks like (for a recent review, see, e.g., [19] and references therein). However, in step with the gradual shift in focus over the last two decades, toward higher- $p_{\perp}$  (“maximum-bias”) physics, the field of QCD entered a golden age of perturbative calculations and infrared safety, during which time the unsafe “soft” physics became viewed increasingly as a nonperturbative quagmire, into the depths of which ventured only fools and old men.

From the perspective of the author’s generation, it was chiefly with a comprehensive set of measurements carried out by Field using the CDF detector at the Tevatron [20–25] that this perception began to change back toward one of a definable region of particle production that can be subjected to rigorous scrutiny in a largely model-independent way, and an ambitious program of such measurements is now being drawn up for the LHC experiments. In other words, a well-defined experimental laboratory has been prepared and is now ready for the testing of theoretical models.

Simultaneously with the LHC efforts, it is important to remember that interesting connections are also being explored toward other, related, fields, such as cosmic ray fragmentation (related to forward fragmentation at the LHC) and heavy-ion physics (related to collective phenomena in hadron-hadron interactions). A nice example of this interplay is given, for instance, by the EPOS model [26], which originated in the heavy-ion community, but uses a parton-based model as input and whose properties in the context of ultra-high-energy cosmic ray fragmentation are currently being explored [27,28]. Also methods from the field of numerical optimization are being applied to Monte Carlo tuning (cf., e.g., the Professor [29] and Profit [30] frameworks), and there are tempting connections back to perturbative QCD. Along the latter vein, we believe that by bringing the logarithmic accuracy of perturbative parton-shower calculations under better control, there would be less room for playing out ambiguities in the nonperturbative physics against ambiguities on the shower side, and hence the genuine soft physics could also be revealed more clearly. This is one of the main motivations behind the VINCIA project [31,32].

For the present, as part of the effort to prepare for the LHC era and spur more interplay between theorists and experimentalists, we shall here report on a new set of tunes of the  $p_{\perp}$ -ordered PYTHIA framework, which update and supersede the older “S0” family [33–36]. We have focused, in particular, on the scaling from lower energies toward the LHC (see also [37–40]) and on attempting to provide at least some form of theoretical uncertainty estimates, represented by a small number of alternate parameter sets that systematically explore variations in some of the main tune parameters. The full set of new tunes have been made available starting from PYTHIA version 6.4.23 (though some have been available longer; see the PYTHIA update notes [41] for details). Based on these variations, we make a best-guess prediction of the charged-track multiplicity in inelastic, nondiffractive events at LHC (cf. Sec. V, Table I).

This concludes a several-year long effort to present the community with an optimized set of parameters that can be used as default settings for the so-called “new” interleaved shower and underlying-event model in PYTHIA 6. The author’s intention is to now move fully to the development of

PYTHIA 8. We note that the Perugia tunes can unfortunately not be used directly in PYTHIA 8, since it uses slightly different parton-shower and color-reconnection models. A separate set of tunes for PYTHIA 8 are therefore under development, with several already included in the current version 8.1.42 of that generator.

We also present a few distributions that carry interesting information about the underlying physics, updating and complementing those contained in [36,42]. For brevity, this text only includes a representative selection, with more results available on the Web [43].

The main point is that, while any plot of an infrared sensitive quantity represents a complicated cocktail of physics effects, such that any sufficiently general model presumably could be tuned to give an acceptable description observable by observable, it is very difficult to simultaneously describe the entire set. The real game is therefore not to study one distribution in detail, for which a simple fit would in principle suffice, but to study the degree of simultaneous agreement or disagreement over many, mutually complementary, distributions.

## II. PROCEDURE

### A. Manual vs automated tuning

Although Monte Carlo models may appear to have a bewildering array of independently adjustable parameters, it is worth keeping at the front of one's mind that most of these parameters only control relatively small (exclusive) details of the event generation. The majority of the (inclusive) physics is determined by only a few, very important ones, such as, e.g., the value of the strong coupling, in the perturbative domain, and the form of the fragmentation function for massless partons, in the nonperturbative one.

#### 1. Manual tuning

Armed with a good understanding of the underlying model, and using only the generator itself as a tool, a generator expert would therefore normally take a highly factorized approach to constraining the parameters, first constraining the perturbative ones and thereafter the non-perturbative ones, each ordered in a measure of their relative significance to the overall modeling. This factorization, and carefully chosen experimental distributions corresponding to each step, allows the expert to concentrate on just a few parameters and distributions at a time, reducing the full parameter space to manageable-sized chunks. Still, each step will often involve more than one single parameter, and nonfactorizable corrections still imply that changes made in subsequent steps can change the agreement obtained in previous ones by a non-negligible amount, requiring additional iterations from the beginning to properly tune the entire generator framework.

Because of the large and varied data sets available, and the high statistics required to properly explore tails of

distributions, mounting a proper tuning effort can therefore be quite intensive—often involving testing the generator against the measured data for thousands of observables, collider energies, and generator settings. Although we have not kept a detailed record, an approximate guess is that the generator runs involved in producing the particular tunes reported on here consumed on the order of 1.000.000 CPU hours, to which can be added an unknown number of man hours. While some of these man hours were undoubtedly productive, teaching the author more about his model and resulting in some of the conclusions reported on in this paper, most of them were merely tedious, while still disruptive enough to prevent getting much other work done.

The main steps followed in the tuning procedure for the Perugia tunes are described in more detail in Sec. II B.

#### 2. Automated tuning

As mentioned in the Introduction, recent years have seen the emergence of automated tools that attempt to reduce the amount of both computer and manpower required. The number of machine hours can, for instance, be substantially reduced by making full generator runs only for a limited set of parameter points, and then interpolating between these to obtain approximations to what the true generator result would have been for any intermediate parameter point. In the Professor tool [29,44], which we rely on for our LEP tuning here, this optimization technique is used heavily, so that after an initial (intensive) initialization period, approximate generator results for *any* set of generator parameters within the sampled space can be obtained without any need of further generator runs. Taken by itself, such optimization techniques could in principle also be used as an aid to manual tuning, but Professor, and other tools such as Profit [30], attempt to go a step further.

Automating the human expert input is of course more difficult (so the experts believe). What parameters to include, in what order, and which ranges for them to consider “physical”? What distributions to include, over which regions, how to treat correlations between them, and how to judge the relative importance, for instance, between getting the right average of an observable versus getting the right asymptotic slope? In the tools currently on the market, these questions are addressed by a combination of input solicited from the generator authors (e.g., which parameters and ranges to consider, which observables constitute a complete set, etc.) and the elaborate construction of nontrivial weighting functions that determine how much weight is assigned to each individual bin and to each distribution. The field is still burgeoning, however, and future sophistications are to be expected. Nevertheless, at this point the overall quality of the tunes obtained with automated methods appear to the author to at least be competitive with the manual ones.

## B. Sequence of tuning steps

We have tuned the Monte Carlo in five consecutive steps:

- (1) Final-state radiation (FSR) and hadronization (HAD): using LEP data [45,46]. For most of the Perugia tunes, we take the LEP parameters given by the Professor Collaboration [29,44]. This improves several event shapes and fragmentation spectra as compared to the default settings. For hadronic yields, especially  $\phi^0$  was previously wrong by more than a factor of 2, and  $\eta$  and  $\eta'$  yields have likewise been improved. For a “HARD” and a “SOFT” tune variation, we deliberately change the renormalization scale for FSR slightly away from the central Professor value. Also, since the Professor parameters were originally optimized for the  $Q^2$ -ordered parton shower in PYTHIA, the newest (2010) Perugia tune goes slightly further, by changing the other fragmentation parameters (by order of 5%–10% relative to their Professor values) in an attempt to improve the description of high- $z$  fragmentation and strangeness yields reported at LEP [45,46] and at RHIC [47,48], relative to the Professor  $p_\perp$ -ordered tuning. The amount of ISR jet broadening (i.e., FSR off ISR) in hadron collisions has also been increased in Perugia 2010, relative to Perugia 0, in an attempt to improve hadron collider jet shapes and rates [49,50].
- (2) Initial-state radiation (ISR) and primordial  $k_T$ : using the Drell-Yan  $p_\perp$  spectrum at 1800 and 1960 GeV, as measured by CDF [51] and D0 [52], respectively. Note that we treat the data as fully corrected for photon bremsstrahlung effects in this case, i.e., we compare the measured points to the Monte Carlo distribution of the “original Z boson.” We are aware that this is not a physically meaningful observable definition, but believe it is the closest we can come to the definition actually used for the data points in both the CDF and D0 studies. See [53] for a more detailed discussion of this issue. Again, we deliberately change the renormalization scale for ISR away from its best fit value for the HARD and SOFT variations, by about a factor of 2 in either direction, which does not appear to lead to serious conflict with the data (see distributions below).
- (3) Underlying event (UE), beam remnants (BR), and color Reconnections (CR): using  $N_{\text{ch}}$  [54,55],  $dN_{\text{ch}}/dp_\perp$  [56,57], and  $\langle p_\perp \rangle(N_{\text{ch}})$  [57] in min-bias events at 1800 and 1960 GeV, as measured by CDF. Note that the  $N_{\text{ch}}$  spectrum extending down to zero  $p_\perp$  measured by the E735 Collaboration at 1800 GeV [58] was left out of the tuning, since we were not able to consolidate this measurement with the rest of the data. We do not know whether this is

due to intrinsic limitations in the modeling (e.g., mismodeling of the low- $p_\perp$  and/or high- $\eta$  regions, which are included in the E735 result but not in the CDF one) or to a misinterpretation on our part of the measured observable. Note, however, that the E735 Collaboration itself remarks [58] that its results are inconsistent with those reported by UA5 [59,60] over the entire range of energies where both experiments have data. So far, the early LHC results at 900 GeV appear to be consistent with UA5, within the limited  $\eta$  regions accessible to the experiments [61–63], but it remains important to check the high-multiplicity tail in detail, in as large a phase space region as possible. We also note that there are some discrepancies between the CDF run-1 [54] and run-2 [55] measurements at very low multiplicities, presumably due to ambiguities in the procedure used to correct for diffraction. We have here focused on the high-multiplicity tail, which is consistent between the two. Hopefully, this question can also be addressed by comparisons to early low-energy LHC data. Although the 4 main LHC experiments are not ideal for diffractive studies and cannot identify forward protons, it is likely that a good sensitivity can still be obtained by requiring events with large rapidity gaps, where the gap definition would essentially be limited by the noise levels achievable in the electromagnetic calorimeters.

- (4) Energy scaling: using  $N_{\text{ch}}$  in min-bias events at 200, 546, and 900 GeV, as measured by UA5 [59,60], and at 630 and 1800 GeV, as measured by CDF [54].
- (5) The last two steps were iterated a few times.

## C. Remarks on jet universality

Note that the clean separation between the first and second points in the list above assumes jet universality, i.e., that a  $Z^0$ , for instance, fragments in the same way at a hadron collider as it did at LEP. This is not an unreasonable first assumption [64], but since the infrared environment in hadron collisions is characterized by a different (hadronic) initial-state vacuum, by a larger final-state gluon component, and also by simply having a lot more color flowing around in general, it is still important to check to what precision it holds explicitly, e.g., by measuring multiplicity and  $p_\perp$  spectra of identified particles, particle-particle correlations, and particle production ratios (e.g., strange to unstrange, vector to pseudoscalar, baryon to meson, etc.) *in situ* at hadron colliders. We therefore very much encourage the LHC experiments not to blindly rely on the constraints implied by LEP, but to construct and publish their own full-fledged sets of fragmentation constraints using identified particles. This is the only way to verify explicitly to what extent the models extrapolate correctly to the LHC environment, and gives the possibility to highlight and address any discrepancies.

### D. Remarks on diffraction

Note also that the modeling of diffraction in PYTHIA 6 lacks a dedicated modeling of diffractive jet production, and hence we include neither elastic nor diffractive Monte Carlo events in any of our comparisons. This affects the validity of the modeling for the first few bins in multiplicity. Due also to the discrepancy noted above between the two CDF measurements in this region [54,55], we therefore assigned less importance to these bins when doing the tunes.<sup>2</sup> We emphasize that widespread use of ill-defined terminologies such as “nonsingle diffractive” (NSD) events without an accompanying definition of what is meant by that terminology at the level of physical observables contributes to the ambiguities surrounding diffractive corrections in present data sets. Since different diffraction models produce different spectra at the observable level, an intrinsic ambiguity is introduced which was not present in the raw data. We strongly encourage future measurements if not to avoid such terminologies entirely then to at least *also* make data available in a form which is defined only in terms of physical observables, i.e., using explicit cuts, weighting functions, and/or trigger conditions to emphasize the role of one component over another.

### E. Remarks on observables

Finally, note that we did not include any explicit underlying-event observables in the tuning. Instead, we rely on the large-multiplicity tail of minimum-bias events to mimic the underlying event. A similar procedure was followed for the older “S0” tune [33,34], which gave a very good simultaneous description of underlying-event physics at the Tevatron.<sup>3</sup> Conversely, Field’s “Tune A” [38,65] gave a good simultaneous description of minimum-bias data, despite only having been tuned on underlying-event data. Tuning to one and predicting the other is therefore not only feasible but simultaneously a powerful cross-check on the universality properties of the modeling.

Additional important quantities to consider for further model tests and tuning would be event shapes at hadron colliders [50,66], observables involving explicit jet reconstruction—including so-called “charged jets” [21] (a jet algorithm run on a set of charged tracks, omitting neutral energy), which will have fluctuations in the charged-to-neutral ratio overlaid on the energy flow and therefore will be more IR than full jets, but still less so than individual particles, and “EM jets” (a jet algorithm run on a set of charged tracks plus photons), which basically adds back

<sup>2</sup>To ensure an apples-to-apples comparison for the low-multiplicity bins between these models and present measurements, one must take care to include any relevant diffractive components using a (separate) state-of-the-art modeling of diffraction.

<sup>3</sup>Note: when extrapolating to lower energies, the alternative scaling represented by “S0A” appears to be preferred over the default scaling used in “S0.”

the  $\pi^0$  component to the charged jets and hence is less IR sensitive than pure charged jets while still remaining free of the noisy environment of hadron calorimeters—explicit underlying-event, fragmentation, and jet structure (e.g., jet mass, jet shape, jet-jet separation) observables in events with jets [6,20–24,49,67–72], photon + jet(s) events (including the important  $\gamma$  + 3-jet signature for double-parton interactions [8,10]), Drell-Yan events [20,72,73], and observables sensitive to the initial-state shower evolution in deep inelastic scattering (DIS) (see, e.g., [37,74]).

As mentioned above, it is also important that fragmentation models tuned at LEP be tested *in situ* at hadron colliders. To this effect, single-particle multiplicities and momentum spectra for identified particles such as  $K_S^0$ , vector mesons, protons, and hyperons (in units of GeV and/or normalized to a global measure of transverse energy, such as, e.g., the  $p_\perp$  of a jet when the event is clustered back to a dijet topology) are the first order of business, and particle-particle correlations the second (e.g., how charge, strangeness, baryon number, etc., are compensated as a function of a distance measure and how the correlation strength of particle production varies over the measured phase space region). Again, these should be considered at the same time as less infrared sensitive variables measuring the overall energy flow. We expect a program of such measurements to gradually develop as it becomes possible to extract more detailed information from the LHC data and note that some such observables, from earlier experiments, have already been included, e.g., in the Rivet framework, see [29], most notably underlying-event observables from the Tevatron, but also recently some fragmentation spectra from RHIC [47,48]. See also the underlying-event sections in the HERA-and-the-LHC [37], Tevatron-for-LHC [38], and Les Houches write-ups [39]. A complementary and useful guide to tuning has been produced by the ATLAS Collaboration in the context of their MC09 tuning efforts [75].

## III. MAIN FEATURES OF THE PERUGIA TUNES

Let us first describe the overall features common to all the Perugia tunes, divided into the same main steps as in the outline of the tuning procedure given in the preceding section: (1) final-state radiation and hadronization, (2) initial-state radiation and primordial  $k_T$ , (3) underlying event, beam remnants, and color reconnections, and (4) energy scaling. Each step will be accompanied by plots to illustrate salient points and by a summary table in Appendix A giving the Perugia parameters relevant to that step, as compared to the older Tune S0A-Pro, which serves as our reference. We shall then turn to the properties of the individual tunes in the following section, and finally to extrapolations to the LHC in the last section.

### A. Final-state radiation and hadronization (Table II)

As mentioned above, we have taken the LEP tune obtained by the Professor group [29,44] as our starting point

for the FSR and HAD parameters for the Perugia tunes. Since we did not perform this part of the tuning ourselves, we treat these parameters almost as fixed inputs, and only a very crude first attempt at varying them was originally made for the Perugia HARD and SOFT variations. This is reflected in the relatively small differences between the FSR and HAD parameters listed in Table II, compared to S0A-Pro which uses the original Professor parameters. (For example, most of the tunes use the same parameters for the longitudinal fragmentation function applied in the string hadronization process, including the same Lund functions [76] for light quarks and Bowler functions [77] for heavy quarks.) With the most recent Perugia 2010 tune, an effort was made to manually improve jet shapes, strangeness yields, and high- $z$  fragmentation, which is the reason several of the hadronization parameters differ in this tune as well as in its sister tune Perugia K. A more systematic exploration of variations in the fragmentation parameters is certainly a point to return to in the future, especially in light of the new identified-particle spectra and jet shape data that will hopefully soon be available from the LHC experiments. For the present, we have focused on the uncertainties in the hadron-collider-specific parameters, as follows.

**B. Initial-state radiation and primordial  $k_T$  (Table III)**

*1. Evolution variable, kinematics, and renormalization scale*

One of the most significant changes when going from the old (virtuality-ordered) to the new ( $p_\perp$ -ordered) ISR/FSR model concerns the Drell-Yan  $p_\perp$  spectrum. In the old model, when an originally massless ISR parton evolves to become a jet with a timelike invariant mass, then that

original parton is pushed off its mass shell by reducing its momentum components. In particular, the transverse-momentum components are reduced, and hence each final-state emission off an ISR parton effectively removes  $p_\perp$  from that parton, and by momentum conservation also from the recoiling Drell-Yan pair. Via this mechanism, the  $p_\perp$  distribution generated for the Drell-Yan pair is shifted toward lower values than what was initially produced.

Compared to data, this appears to effectively cause any tune of the old PYTHIA framework with default ISR settings—such as Tune A or the ATLAS DC2/“Rome” tune—to predict a too narrow spectrum for the Drell-Yan  $p_\perp$  distribution, as illustrated by the comparison of Tune A to CDF and D0 data in Fig. 1 (left column). (The inset shows the high- $p_\perp$  tail which in all cases is matched to  $Z + \text{jet}$  matrix elements, the default in PYTHIA for both the virtuality- and  $p_\perp$ -ordered shower models.) We note that a recent theoretical study [78] using virtuality ordering with a different kinematics map did not find this problem, consistent with our suspicion that it is not the virtuality ordering *per se* which results in the narrow shape, but the specific recoil kinematics of FSR off FSR in the old shower model.

To reestablish agreement with the measured spectrum without changing the recoil kinematics, the total amount of ISR in the old model had to be increased. This can be accomplished, e.g., by choosing very low values of the renormalization scale (and hence large  $\alpha_s$  values) for ISR, as illustrated by tunes DW-Pro and Pro-Q2O in Fig. 1 (left column). To summarize, the  $\alpha_s$  choices corresponding to each of the three tunes of the old shower shown in the left pane of Fig. 1 are

$$Q^2 \text{ ordering } \left\{ \begin{array}{l} \text{Tune A (100)} \\ \text{Tune DW (103)} \\ \text{Tune Pro-Q2O (129)} \end{array} \right. : \begin{array}{l} \alpha_s(p_\perp^2) \quad \overline{\text{MS}}, \quad 1\text{-loop}, \quad \Lambda_{\text{CTEQ5L}}, \\ \alpha_s(0.2p_\perp^2) \quad \overline{\text{MS}}, \quad 1\text{-loop}, \quad \Lambda_{\text{CTEQ5L}}, \\ \alpha_s(0.14p_\perp^2) \quad \overline{\text{MS}}, \quad 1\text{-loop}, \quad \Lambda_{\text{CTEQ5L}}, \end{array} \quad (3)$$

where, for completeness, we have given also the renormalization scheme, loop order, and choice of  $\Lambda_{\text{QCD}}$ , which are the same for all the tunes.

While the increase of  $\alpha_s$  nominally reestablishes a good agreement with the Drell-Yan  $p_\perp$  spectrum, the whole business does smell faintly of fixing one problem by introducing another and hence the defaults in PYTHIA for these parameters have remained the Tune A ones, at the price of retaining the poor agreement with the Drell-Yan spectrum.

In the new  $p_\perp$ -ordered showers [12], however, FSR off ISR is treated within individual QCD dipoles and does not affect the Drell-Yan  $p_\perp$ . This appears to make the spectrum come out generically much closer to the data, as illustrated by the S0(A) curves in Fig. 1 (right column), which use  $\alpha_s(p_\perp)$ . The only change going to Perugia 0—which can be seen to be slightly harder—was implementing a

translation from the  $\overline{\text{MS}}$  definition of  $\Lambda$  used previously, to the so-called CMW choice [79] for  $\Lambda$ , similarly to what is done in HERWIG [80,81].

For both CTEQ5L and CTEQ6L1, the  $\Lambda_{\text{QCD}}^{\overline{\text{MS}}}$  value in the parton distribution function (PDF) set is derived with an LO (1-loop) running of  $\alpha_s$ , which is also what we use in the backward evolution algorithm in our ISR model. In the Perugia tunes (and also in PYTHIA by default) we therefore let the  $\alpha_s$  value for the ISR evolution be determined by the PDF set, which is the main reason the PDF choice appears in the list of ISR parameters in Table III. The MRST LO\* set [82], however, uses a next-to-leading order (NLO) (2-loop) running for  $\alpha_s$ , which gives a roughly 50% larger value for  $\Lambda$ . Since we do not change the loop order of our ISR evolution, this higher  $\Lambda$  value in turn leads to an increase of roughly 5% in the mean Drell-Yan  $p_\perp$  at the

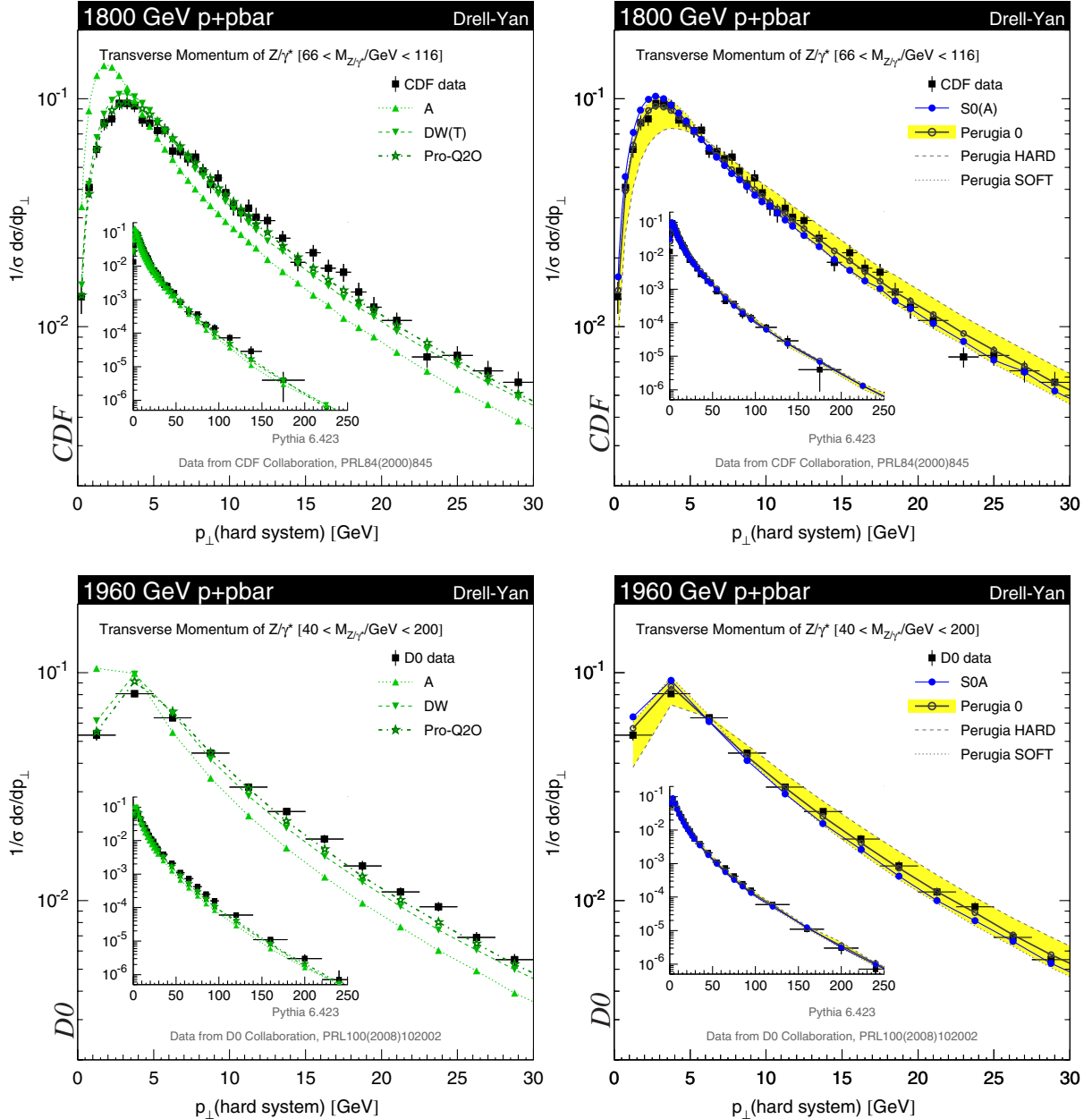


FIG. 1 (color online). Comparisons to the CDF and D0 measurements of the  $p_{\perp}$  of Drell-Yan pairs [51,52]. Insets show the high- $p_{\perp}$  tails. Left panels: virtuality-ordered showers. Right panels:  $p_{\perp}$ -ordered showers. See [43] for other tunes and collider energies.

Tevatron (as compared to virtually no change between CTEQ5L and CTEQ6L1 despite a 10% change in  $\Lambda$  between those two). To compensate for the higher  $\Lambda$  value, which we regard as an artifact of the incompatibility between the loop order of the LO\* set and that of our ISR shower, the renormalization scale was therefore chosen slightly higher for the LO\* tune, cf. the PARP (64) values in Table III, effectively translating it back to a value more appropriate for a 1-loop running. We note that a similar issue afflicted the original CTEQ6L set, which used an NLO  $\alpha_s$ , with a correspondingly larger value of  $\Lambda$ . We here use the revised CTEQ6L1 set for our Perugia 6 tune, which uses an LO running. Similarly, the LO\* set

used here could be replaced by the newer LO\*\* one, which uses an LO  $\alpha_s$ , but this was not yet available at the time our LO\* tune was performed. The main reason for sticking to CTEQ5L for Perugia 0 was the desire that this tune can be run with stand-alone PYTHIA 6. We note that in PYTHIA 8, several more recent sets have already been implemented in the stand-alone version [83], hence removing this restriction from corresponding tuning efforts for PYTHIA 8.

Finally, the HARD and SOFT variations shown by the yellow (shaded) band in the right pane of Fig. 1 are obtained by making a variation of roughly a factor of 2 in either direction from the central tune (in the case of the SOFT tune, this is obtained by a combination of reverting to the

$\overline{MS}$  value for  $\Lambda$  and using  $\sqrt{2}p_{\perp}$  as the renormalization scale). In the low- $p_{\perp}$  peak, the HARD variation generates a slightly too broad distribution, but given the large sensitivity of this peak to subleading corrections (see below), we consider this to be consistent with the expected theoretical precision. The  $p_{\perp}$  spectrum of the other Perugia tunes will be covered in the section on the individual tunes below.

## 2. Phase space

A further point concerning ISR that deserves discussion is the phase space over which ISR emissions are allowed. Here, Drell-Yan is a special case, since this process is matched to  $Z + \text{jet}$  matrix elements in PYTHIA [84,85], and hence the hardest jet is always described by the matrix element over all of phase space. For unmatched processes which do not contain jets at leading order, the fact that we start the parton shower off from the factorization scale can, however, produce an illusion of almost zero jet activity above that scale. This was studied in [86,87], where also the consequences of dropping the phase space cutoff at the factorization scale were investigated, so-called power showers. Our current best understanding is that the conventional (“wimpy”) showers with a cutoff at the factorization scale certainly underestimate the tail of ultrahard emissions while the power showers are likely to overestimate it, hence making the difference between the two a useful measure of uncertainty. Since other event generators usually provide wimpy showers by default, we have chosen to give the power variants as the default in PYTHIA 6—not because the power shower approximation is necessarily better, but simply to minimize the risk that an accidental agreement between two generators is taken as a sign of a

small overall uncertainty, and also to give a conservative estimate of the amount of hard additional jets that can be expected. Note that a more systematic description of hard radiation that interpolates between the power and wimpy behaviors has recently been implemented in PYTHIA 8 [88].

For the Perugia models, we have implemented a simpler possibility to smoothly dampen the tail of ultrahard radiation, using a scale determined from the color flow as reference. This is done by nominally applying a power shower, but dampening it by a factor

$$P_{\text{accept}} = P_{67} \frac{s_D}{4p_{\perp, \text{evol}}^2}, \quad (4)$$

where  $P_{67}$  corresponds to the parameter `PARP(67)` in the code,  $p_{\perp, \text{evol}}^2$  is the evolution scale for the trial splitting, and  $s_D$  is the invariant mass of the radiating parton with its color neighbor, with all momenta crossed into the final state (i.e., it is  $\hat{s}$  for annihilation-type color flows and  $-\hat{t}$  for an initial-final connection). This is motivated partly by the desire to give an intermediate possibility between the pure power and pure wimpy options but also partly from findings that similar factors can substantially improve the agreement with final-state matrix elements in the context of the VINCIA shower [32]. By default, the Perugia tunes use a value of 1 for this parameter, with the SOFT and HARD tunes exploring systematic variations; see Table III.

At the Tevatron, the question of power vs wimpy showers is actually not much of an issue, since  $H/V + \text{jets}$  is already matched to matrix elements in default PYTHIA and most other interesting processes either contain QCD jets already at leading order [ $\gamma + \text{jets}$ , dijets, weak boson fusion (WBF)] or have very little phase space for radiation

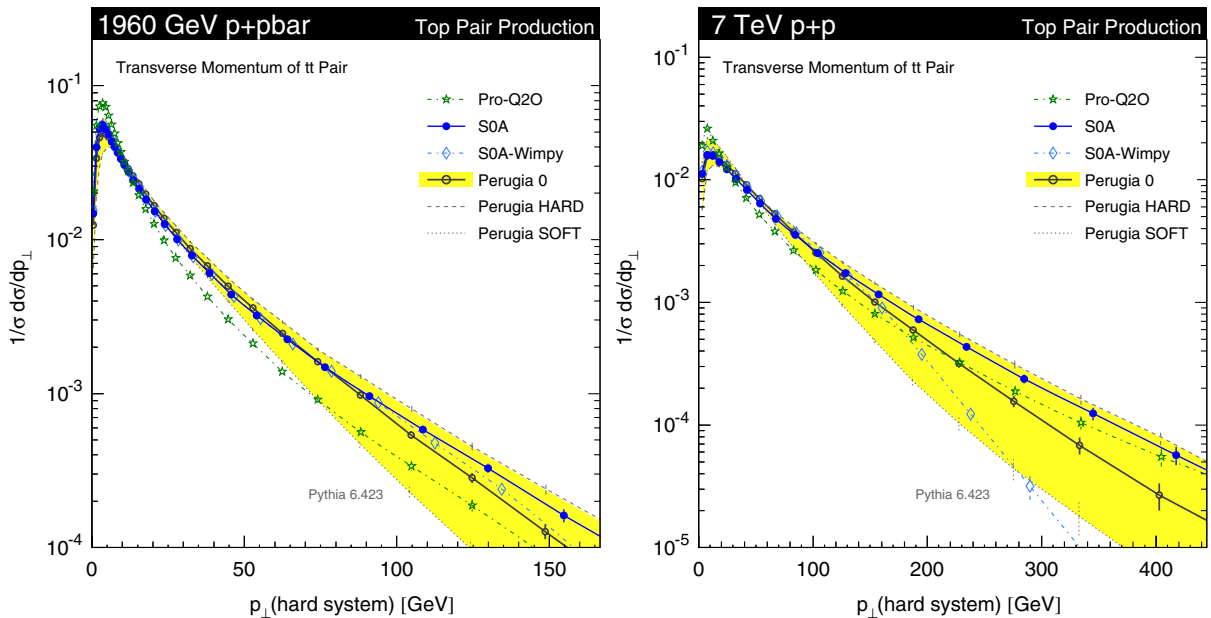


FIG. 2 (color online). Comparison of new and old tunes for the  $p_{\perp}$  of  $t\bar{t}$  pairs at the Tevatron (left panel) and at the LHC at 7 TeV (right panel). See [43] for other tunes and collider energies.



above the factorization scale anyway ( $t\bar{t}$ , dibosons). This is illustrated by the curves labeled S0A (solid blue line) and S0A-Wimpy (dash-dotted cyan line) in the left pane of Fig. 2, which shows the  $p_\perp$  spectrum of the  $t\bar{t}$  system (equivalent to the Drell-Yan  $p_\perp$  shown earlier). The two curves do begin to diverge around the top mass scale, but in light of the limited statistics available at the Tevatron, matching to higher-order matrix elements to control this ambiguity does not appear to be of crucial importance. In contrast, when we extrapolate to  $pp$  collisions at 7 TeV, shown in the right pane of Fig. 2, the increased phase space makes the ambiguity larger. Matching to the proper matrix elements describing the region of jet emissions above  $p_\perp \sim m_t$  may therefore be correspondingly more important; see, e.g., [89]. Note that the extremal Perugia variations span most of the full power/wimpy difference, as desired, while the central ones fall in between. Note also that this only concerns the  $p_\perp$  spectrum of the hard jets—power showers cannot in general be expected to properly capture jet-jet correlations, which are partly generated by polarization effects not accounted for in this treatment.

### 3. Primordial $k_T$

Finally, it is worth remarking that the peak region of the Drell-Yan  $p_\perp$  spectrum is extremely sensitive to infrared effects. On the experimental side, this means, e.g., that the treatment of QED corrections can have significant effects and that care must be taken to deal with them in a consistent and model-independent manner [53]. On the theoretical side, relevant infrared effects include whether the low- $p_\perp$  divergences in the parton shower are regulated by a sharp cutoff or by a smooth suppression (and in what

variable), how  $\alpha_s$  is treated close to the cutoff, and how much “Fermi motion” is given to each of the shower-initiating partons extracted from the protons. A full exploration of these effects probably goes beyond what can meaningfully be studied at the current level of precision. Our models therefore only contain one infrared parameter (in addition to the infrared regularization scale of the shower), called “primordial  $k_T$ ,” which should be perceived of as lumping together an inclusive sum of unresolved effects below the shower cutoff. Since the cutoff is typically in the range 1–2 GeV, we do not expect the primordial  $k_T$  to be much larger than this number, but there is also no fundamental reason to believe it should be significantly smaller. This is in contrast to previous lines of thought, which drew a much closer connection between this parameter and Fermi motion, which is expected to be only a few hundred MeV. In Tune A, the value of primordial  $k_T$ , corresponding to PARP(91) in the code, was originally 1 GeV, whereas it was increased to 2.1 GeV in Tune DW. In the Perugia tunes, it varies in the same range; cf. Table III. Its distribution is assumed to be Gaussian in all the models. Explicit attempts exploring alternative distributions in connection with the writeup of this paper [ $1/k_T^6$  tails and even a flat distribution with a cutoff, see [14], MSTP(91)] did not lead to significant differences.

## C. Underlying-event, beam remnants, and color reconnections (Table IV)

### 1. Charged multiplicity

The charged particle multiplicity ( $N_{\text{ch}}$ ) distributions for minimum-bias events at 1800 and 1960 GeV at the Tevatron are shown in Fig. 3. Particles with  $c\tau \geq 10$  mm

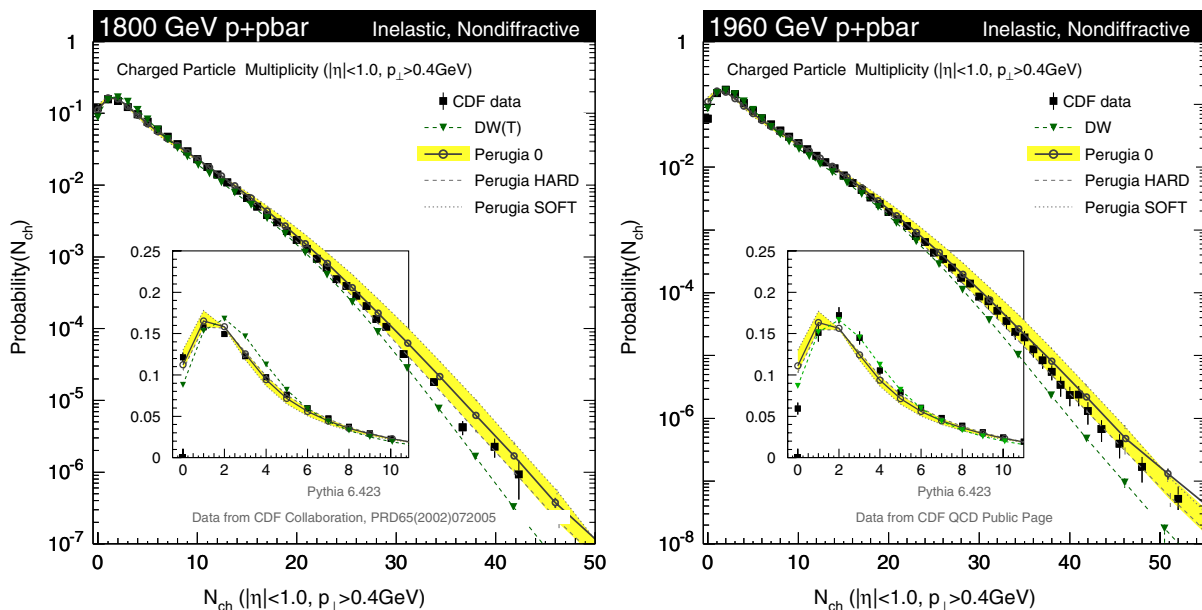


FIG. 3 (color online). Comparisons to the CDF measurements of the charged track multiplicity at 1800 (left panel) and 1960 GeV (right panel) in minimum-bias  $p\bar{p}$  collisions. See [43] for other tunes and collider energies.

$(\mu^\pm, \pi^\pm, K_S^0, K_L^0, n^0, \Lambda^0, \Sigma^\pm, \Xi^0, \Xi^\pm, \text{ and } \Omega^\pm)$  are treated as stable. Models include the inelastic, nondiffractive component only. Note that the Perugia tunes included this data in the tuning, while DW was only tuned to underlying-event data at the same energies. The overall agreement over the many orders of magnitude spanned by these measurements is quite good. On the large-multiplicity tails, DW appears to give a slightly too narrow distribution. In the low-multiplicity peak (see insets), the Perugia tunes fit the 1800 GeV data set better while DW fits the 1960 GeV data set better. As mentioned above, however, diffractive topologies give large corrections in this region, and so the points shown in the insets were not used to constrain the Perugia tunes.

## 2. Transverse-momentum spectrum

The  $p_\perp$  spectrum of charged particles at 1960 GeV is shown in Fig. 4. Note that both plots in the figure show the same data; only the model comparisons are different.

The plot in the left-hand pane illustrates a qualitative difference between the  $Q^2$ - and  $p_\perp$ -ordered models. Comparing DW to NOCR (a tune of the  $p_\perp$ -ordered model which does not employ color reconnections) we see that the  $p_\perp$  spectrum is generically slightly harder in the new model than in the old one. Color reconnections, introduced in S0A, then act to harden this spectrum slightly more, to the point of marginal disagreement with the data. Finally, when we include the Professor tunes to LEP data, nothing much happens to this spectrum in the old model—compare DW with DW-Pro—whereas the spectrum becomes yet harder in the new one, cf. S0A-Pro, now reaching a level

of disagreement with the data that we have to take seriously. Since the original spectrum out of the box—represented by NOCR—was originally quite similar to that of DW and DW-Pro, our tentative conclusion is that either the revised LEP parameters for the  $p_\perp$ -ordered shower have some hidden problem and/or the color reconnection model is hardening the spectrum too much. For the Perugia tunes, we took the latter interpretation, since we did not wish to alter the LEP tuning. Using a modified color-reconnection model that suppresses reconnections among high- $p_\perp$  string pieces (to be described below), the plot in the right-hand pane illustrates that an acceptable level of agreement with the data has been restored in the Perugia tunes, without modifying the Professor LEP parameters.

For completeness we should also note that there are indications of a significant discrepancy developing in the extreme tail of particles with  $p_\perp > 30$  GeV, where all the models fall below the data, a trend that was confirmed with higher statistics in [90]. This discrepancy also appears in the context of NLO calculations folded with fragmentation functions [91], so it is not a feature unique to the PYTHIA modeling. Though we shall not comment on possible causes for this behavior here (see [92,93] for a critical assessment), the extreme tail of the  $p_\perp$  distribution should therefore be especially interesting to check when high-statistics data from the LHC become available.

## 3. $\langle p_\perp \rangle (N_{\text{ch}})$ and color reconnections

While the multiplicity and  $p_\perp$  spectra are thus, separately, well described by Tune DW, it does less well on

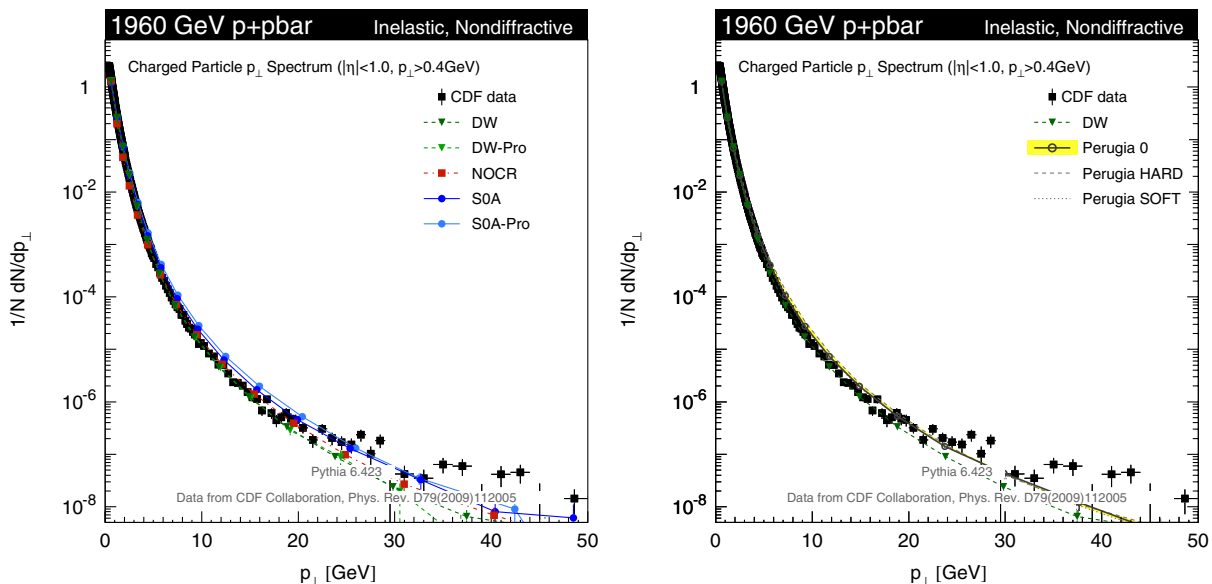


FIG. 4 (color online). Comparisons to the CDF measurement of the charged particle  $p_\perp$  spectrum in minimum-bias  $p\bar{p}$  collisions at 1960 GeV for two sets of models. See [43] for other tunes and collider energies.

their correlation,  $\langle p_{\perp} \rangle(N_{\text{ch}})$ , as illustrated by the plot in the left-hand pane of Fig. 5. Since the S0 family of tunes were initially tuned to Tune A, in the absence of published data, the slightly smaller discrepancy exhibited by Tune A carried over to the S0 set of tunes, as illustrated by the same plot. Fortunately, CDF run-2 data have now been made publicly available [57], corrected to the particle level, and hence it was possible to take the actual data into consideration for the Perugia tunes, resulting in somewhat softer particle spectra in high-multiplicity events; cf. the right-hand pane in Fig. 5.

What is more interesting is how this correlation is achieved by the models. Also shown in the right-hand pane of Fig. 5 are comparisons to an older ATLAS tune which did not use the enhanced final-state color connections that Tunes A and DW employ. A special Perugia variation without color reconnections, Perugia NOCR, is also shown, and one sees that both this and the ATLAS tune predict too little correlation between  $\langle p_{\perp} \rangle$  and  $N_{\text{ch}}$ .

This distribution therefore appears to be sensitive to the color structure of the events, at least within the framework of the PYTHIA modeling [33–35,94]. The Perugia tunes all (with the exception of NOCR) rely on an infrared toy model of string interactions [33] to drive the increase of  $\langle p_{\perp} \rangle$  with  $N_{\text{ch}}$ . The motivation for a model of this type comes from arguing that, in the leading-color limit used by Monte Carlo event generators, and in the limit of many perturbative parton-parton interactions, the central rapidity region in hadron-hadron collisions would be crisscrossed by a very large number of QCD strings: naively one string

per perturbative  $t$ -channel quark exchange, and two per gluon exchange. However, since the actual number of colors is only three, and since the strings would have to be rather closely packed in spacetime, it is not unreasonable to suppose either that the color field collapses in a more economical configuration already from the start, or that the strings undergo interactions among themselves, before the fragmentation process is complete, that tend to minimize their total potential energy, as given by the area law of classical strings. The toy models used by both the S0 and Perugia tunes do not address the detailed dynamics of this process, but instead employ an annealinglike minimization of the total potential energy, where the string-string interaction strength was originally the only variable parameter [33]. While this gave a reasonable agreement with  $\langle p_{\perp} \rangle(N_{\text{ch}})$ , it still tended to give slightly too hard a tail on the single-particle  $p_{\perp}$  distribution, as compared to the Tevatron run-2 measurement. Therefore, a suppression of reconnections among very high- $p_{\perp}$  string pieces was introduced, reasoning that very fast-moving string systems should be able to more easily “escape” the mayhem in the central region. (Similarly, one could argue that string systems produced in the decay of massive particles with finite lifetimes, such as narrow beyond-the-standard-model (BSM) or Higgs resonances, or even possibly hadronic  $t$  or  $W$  decays, should be able to escape more easily. We have not so far built in such a suppression, however.)

The switch MSTP(95) controls the choice of color-reconnection model. In the S0 model corresponding to MSTP(95 = 6) (and = 7 to apply it also in lepton

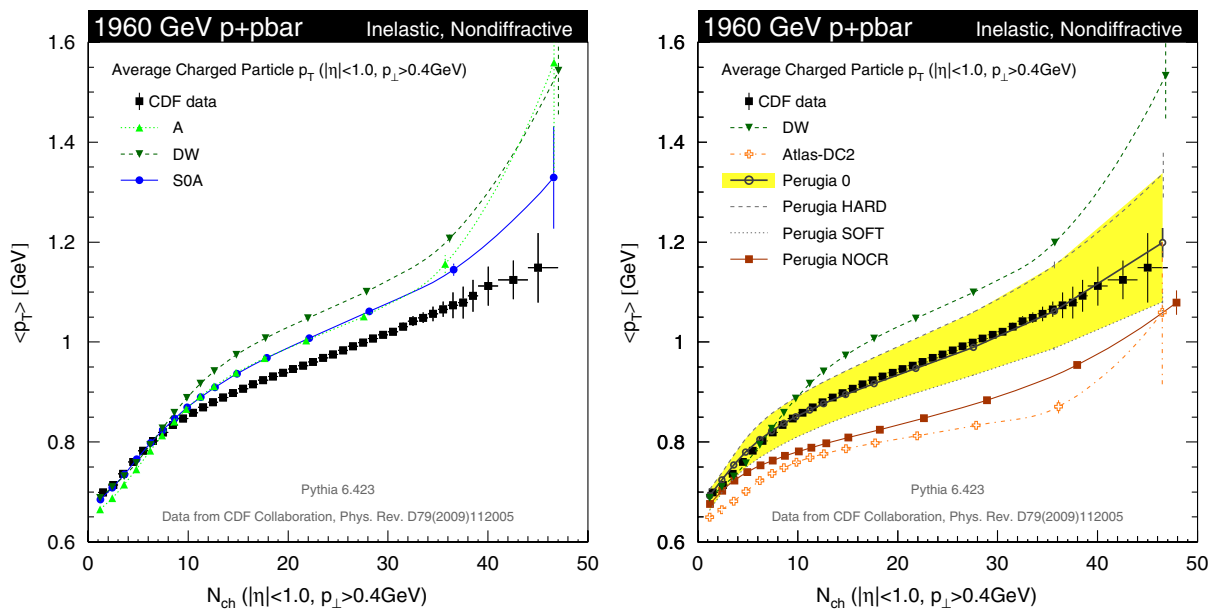


FIG. 5 (color online). Comparisons to the CDF run II measurement of the average track  $p_{\perp}$  as a function of track multiplicity in minibus  $p\bar{p}$  collisions. Left panel: The older generation of tunes. Right panel: the Perugia variations compared to two older tunes. See [43] for other tunes and collider energies.

collisions), the total probability for a string piece to survive the annealing and preserve its original color connections is

$$\text{MSTP}(95) = 6, 7: P_{\text{keep}} = (1 - \zeta P_{78})^{n_{\text{int}}}, \quad (5)$$

where  $P_{78}$  corresponds to the parameter `PARP(78)` in the code and sets the overall color-reconnection strength and  $n_{\text{int}}$  is the number of parton-parton interactions in the current event, giving a rough first estimate of the number of strings spanned between the remnants. (It is thus more likely for a string piece to suffer ‘‘color amnesia’’ in a busy event, than in a quiet one.)  $\zeta$  was introduced together with the Perugia tunes and gives a possibility to suppress reconnections among high- $p_{\perp}$  string pieces,

$$\zeta = \frac{1}{1 + P_{77}^2 \langle p_{\perp} \rangle^2}, \quad (6)$$

with  $P_{77}$  corresponding to `PARP(77)` in the code and  $\langle p_{\perp} \rangle$  being a measure of the average transverse momentum

per pion that the string piece would produce,  $n_{\pi} \propto \ln(s/m_{\pi}^2)$ , with a normalization factor absorbed into  $P_{77}$ .

Starting from PYTHIA 6.4.23, a slightly more sophisticated version of color annealing was introduced, via `MSTP(95) = 8` (and `= 9` to apply it also in lepton collisions), as follows. Instead of using the number of multiple parton-parton interactions to give an average idea of the total number of strings between the remnants, the algorithm instead starts by finding a thrust axis for the event (which normally will coincide with the  $z$  axis for hadron-hadron collisions). It then computes the density of string pieces along that axis, rapidity interval by rapidity interval, with a relatively fine binning in rapidity. Finally, it calculates the reconnection probability for each individual string piece by using the average string density in the region spanned by that string piece, instead of the number of multiple interactions, in the exponent in the above equation:

$$\text{MSTP}(95) = 8, 9: P = (1 - \zeta P_{78})^{\langle n_s \rangle (y_1, y_2)}, \quad (7)$$

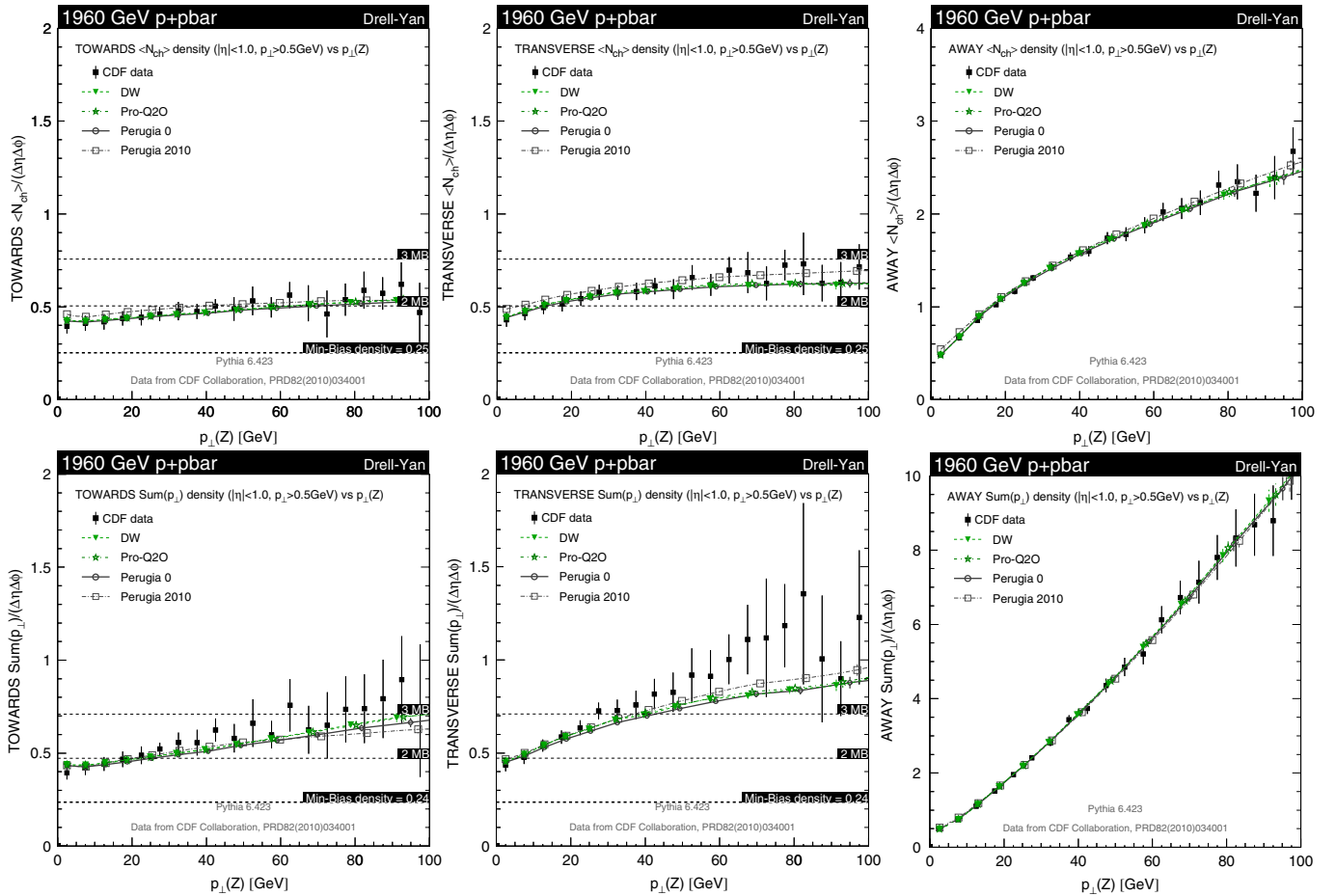


FIG. 6 (color online). Comparisons to the CDF measurements [72,73] of the charged particle multiplicity (top row) and  $p_{\perp}$  (bottom row) densities in the ‘‘TOWARDS’’ (left panels), ‘‘TRANSVERSE’’ (middle panels), and ‘‘AWAY’’ (right panels) regions of Drell-Yan production at 1960 GeV, as a function of the Drell-Yan  $p_{\perp}$ .

where  $\langle n_s \rangle(y_1, y_2)$  is the average number of other string pieces, not counting the piece under consideration, in the rapidity range spanned by the two end points of the piece,  $y_1$  and  $y_2$ . Obviously, the resulting model is still relatively crude—it still has no explicit spacetime picture and hence will not generate more subtle effects such as (elliptical) flow, no detailed dynamics model, and no suppression mechanism for reconnections involving long-lived resonances—but at least the reconnection probability has been made a more local function of the actual string environment, which also provides a qualitative variation on the previous models that can be used to explore uncertainties. In the code, the S0 type is also referred to as the “Seattle” model, since it was written while on a visit there. The newer one is referred to as the “Paquis” type, for similar reasons.

#### 4. Underlying event

In Fig. 6, we show the  $\langle N_{\text{ch}} \rangle$  density<sup>4</sup> (top row) and the  $\langle p_{\perp \text{Sum}} \rangle$  density<sup>5</sup> (bottom row) in each of the TOWARDS, TRANSVERSE, and AWAY regions, for Drell-Yan production at the Tevatron, compared to CDF data [72,73]. The invariant mass window for the lepton pair for this measurement is  $70 < m_{\ell^+\ell^-} < 110$ , in GeV. Tracks with  $p_T > 0.5$  GeV inside  $|\eta| < 1$  were included, with the same definition of stable charged tracks as above. The leptons from the decaying boson were not included.

The agreement between the Perugia min-bias tunes and data is at the same level as that of more dedicated UE tunes, here represented by DW and Pro-Q2, supporting the assertion made earlier concerning the good universality properties of the PYTHIA modeling. We note also that the Perugia 2010 variation agrees slightly better with the data in the TRANSVERSE region, where it has a bit more activity than Perugia 0 does.

#### 5. Transverse mass distribution and MPI showers

Finally, the old framework did not include showering off the multiple-parton-interactions (MPI) in and out states.<sup>6</sup> The new framework does include such showers, which furnish an additional fluctuating physics component. Relatively speaking, the new framework therefore needs *less* fluctuations from other sources in order to describe the same data. This is reflected in the tunes of the new framework generally having a less lumpy proton (smoother proton transverse density distributions) and fewer total numbers of MPI than the old one. This is illustrated in

<sup>4</sup>The  $\langle N_{\text{ch}} \rangle$  density is defined as the average number of tracks per unit  $\Delta\eta\Delta\phi$  in the relevant region.

<sup>5</sup>The  $\langle p_{\perp \text{Sum}} \rangle$  density is defined as the average scalar sum of track  $p_{\perp}$  per unit  $\Delta\eta\Delta\phi$ .

<sup>6</sup>It did, of course, include showers off the primary interaction. An option to include FSR off the MPI also in that framework has since been implemented by Mrenna; see [41], but tunes using that option have not yet been made.

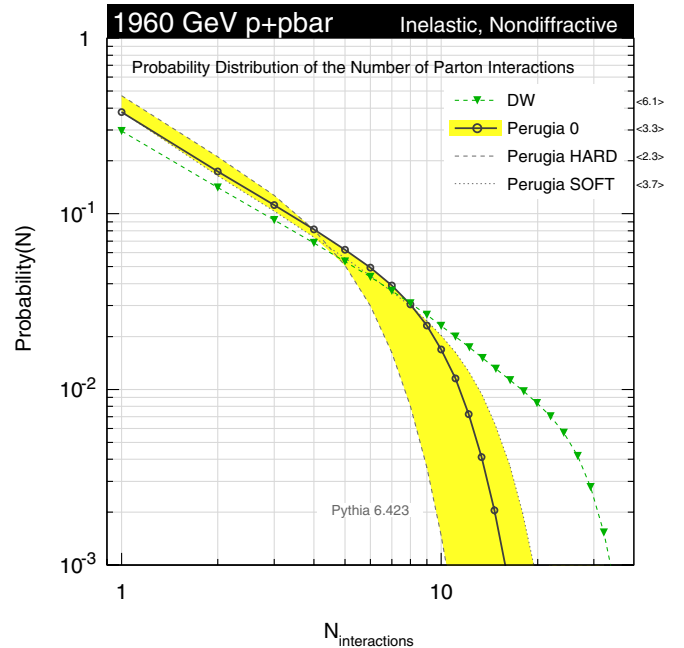


FIG. 7 (color online). Double-logarithmic plot of the probability distribution of the number of parton-parton interactions in min-bias collisions at the Tevatron, showing that the Perugia tunes obtain the same multiplicity distribution, Fig. 3, with fewer MPI than Tune A. See [43] for other tunes and collider energies.

Fig. 7, where a double-logarithmic scale has been chosen in order to reveal the asymptotic behavior more clearly. Note that, e.g., for Tune A, the plot shows that more than a per mil of min-bias events have over 30 perturbative parton-parton interactions per event at the Tevatron. This number is reduced by a factor of 2 to 3 in the new models, while the average number of interactions, indicated on the right-hand side of the plot, goes down by slightly less.

The showers off the MPI also lead to a greater degree of decorrelation and  $p_{\perp}$  imbalance between the minijets produced by the underlying event, in contrast to the old framework where these remained almost exactly balanced and back to back. This should show up in minijet  $\Delta\phi_{jj}$  and/or  $\Delta R_{jj}$  distributions sensitive to the underlying event, such as in  $Z/W + \text{multijets}$  with low  $p_{\perp}$  cuts on the additional jets. It should also show up as a relative enhancement in the odd components of Fourier transforms of  $\phi$  distributions *à la* [95].

#### 6. Long-range correlations

Further, since showers tend to produce shorter-range correlations than MPI, the new tunes also exhibit smaller long-range correlations than did the old models. That is, if there is a large fluctuation in one end of the detector, it is *less* likely in the new models that there is a large fluctuation in the same direction in the other end of the detector. The impact of this on the overall modeling, and on correction

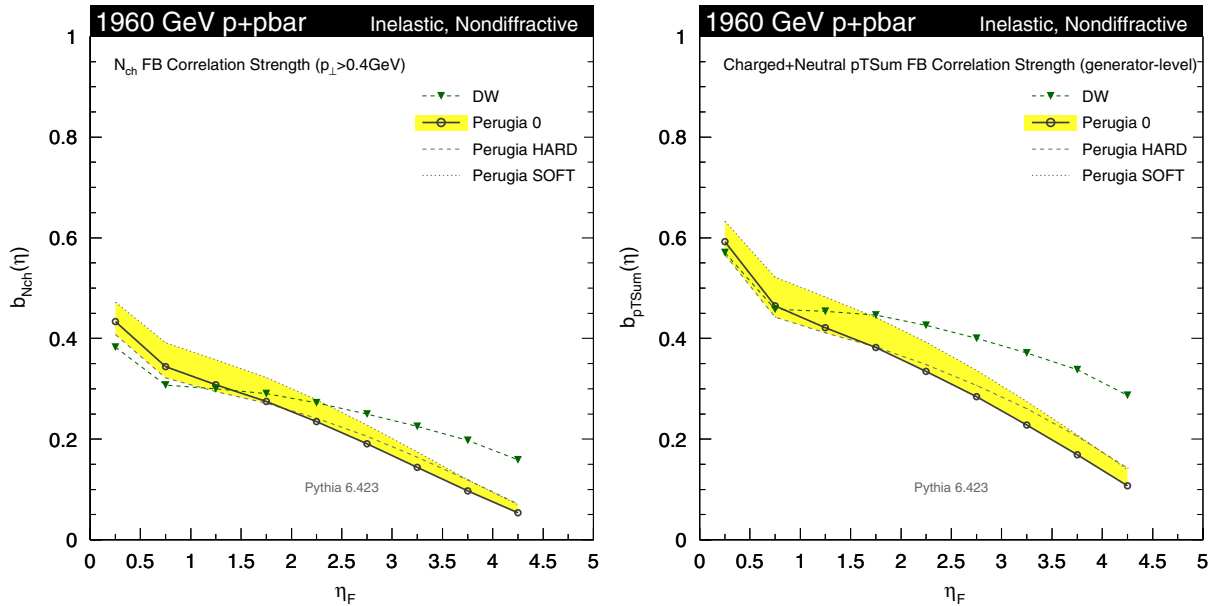


FIG. 8 (color online). Forward-backward correlation strengths at the Tevatron in (left panel) charged particles and (right panel) charged plus neutral transverse-momentum sum at generator level. See [43] for other tunes and collider energies.

procedures derived from it, has not yet been studied in great detail. One variable which can give direct experimental information on the correlation strength over both short and long distances is the so-called forward-backward correlation,  $b$ , defined as in [94,96]

$$b(\eta_F) = \frac{\langle n_F n_B \rangle - \langle n_F \rangle^2}{\langle n_F^2 \rangle - \langle n_F \rangle^2}, \quad (8)$$

where  $n_F$  and  $n_B$  are the number of tracks (or a calorimetric measure of energy deposition) in a pseudorapidity bin centered at  $\eta_F$  and  $\eta_B = -\eta_F$ , respectively, for a given event. The averages indicate averaging over the number of recorded events. The resulting correlation strength,  $b$ , can be plotted either as a function of  $\eta_F$  or as a function of the distance,  $\Delta\eta$ , between the bins. A comparison of the main Perugia tunes to Tune DW is shown in Fig. 8, for two different variants of the correlation strength: the plot on the left only includes charged particles with  $p_\perp > 0.4$  GeV and the other (right) includes all energy depositions (charged plus neutral) that would be recorded by an idealized calorimeter. Since estimating the impact on the latter of a real (noisy) calorimeter environment would go beyond the scope of this paper, we here present the correlation at generator level. For the former, we show the behavior out to  $\eta = 5$  although the CDF and D0 detectors would of course be limited to measuring it inside the region  $|\eta| < 1.0$ . Note that a measurement of this variable would also be a prerequisite for combining the  $dN/d\eta$  measurements from negative and positive  $\eta$  regions to form  $dN/d|\eta|$ , with the proper correlations taken into account. This particular application of the  $b$  measurement would require a

measurement of  $b$  with the same bin sizes as used for  $dN/d\eta$ . Since the amount of correlation depends on the bin size used (smaller bin sizes are more sensitive to uncorrelated fluctuations), we would advise one to perform the  $b$  measurement using several different bin sizes, ranging from a very fine binning (e.g., paralleling that of the  $dN/d\eta$  measurement), to very wide bins (e.g., one unit in pseudorapidity as used in [94]). For our plots here, we used an intermediate-sized binning of 0.5 units in pseudorapidity.

#### D. Energy scaling (Table IV)

A final difference with respect to the older S0(A) family of tunes is that we here include data from different colliders at different energies, in an attempt to fix the energy scaling better.

The energy scaling of min-bias and underlying-event phenomena, in both the old and new PYTHIA models, is driven largely by a single parameter, the scaling power of the infrared regularization scale for the multiple parton interactions,  $p_{\perp 0}$ ; see, e.g., [13,14,94]. This parameter is assumed to scale with the collider c.m. energy squared,  $s$ , in the following way:

$$p_{\perp 0}^2(s) = p_{\perp 0}^2(s_{\text{ref}}) \left( \frac{s}{s_{\text{ref}}} \right)^{P_{90}}, \quad (9)$$

where  $p_{\perp 0}^2(s_{\text{ref}})$  is the IR regularization scale given at a specific reference  $s = s_{\text{ref}}$ , and  $P_{90}$  sets the scaling away from  $s = s_{\text{ref}}$ . In the code,  $p_{\perp 0}^2(s_{\text{ref}})$  is represented by PARP(82),  $\sqrt{s_{\text{ref}}}$  by PARP(89), and  $P_{90}$  by PARP(90). Note that large values of  $P_{90}$  produce a *slower* rate of

increase in the overall activity with collider energy than low values, since the generation of additional parton-parton interactions in the underlying event is suppressed below  $p_{\perp 0}$ .

The default value for the scaling power in PYTHIA 6.2 was  $P_{90} = 0.16$ , motivated [94] by relating it to the scaling of the total cross section, which grows like  $\propto E_{\text{c.m.}}^{0.16}$ . When comparing to Tevatron data at 630 GeV, Field found that this resulted in too little activity at that energy, as illustrated in the top row of Fig. 9, where tune DWT uses the old default scaling away from the Tevatron and DW uses Field's value of  $P_{90} = 0.25$ . (The total cross section is still obtained from a Donnachie-Landshoff fit [97] and is not affected by this change.) Note that the lowest-multiplicity bins of the UA5 data, in particular, and the first bin of the CDF data were ignored for our comparisons here, since these contain a large diffractive component, which has not been simulated in the model comparisons.

For the Perugia tunes, the main variations of which are shown in the bottom row of Fig. 9, we find that a large

range of values, between 0.22 and 0.32, can be accommodated without ruining the agreement with the available data, with Perugia 0 using 0.26.

The energy scaling is therefore still a matter of large uncertainty, and the possibility of getting good additional constraints from the early LHC data is encouraging. The message so far appears to be contradictory, however, with early ATLAS results at 900 GeV [63] appearing to confirm the tendency of the current tunes to undershoot the high-multiplicity tail at 900 GeV (see the right-hand column of Fig. 9), which would indicate a slower scaling between 900 and 1800 GeV than what is generated by the models (since they all fit well at 1800 GeV) but preliminary CMS results on the average multiplicity at 2360 GeV [62] indicate the opposite, that the pace of evolution in the models is actually too slow. Furthermore, the CDF data at 630 GeV and the UA5 data at 200 GeV provide additional constraints at lower energies which have made it difficult for us to increase the tail at 900 GeV without coming into conflict with at least one of these other data

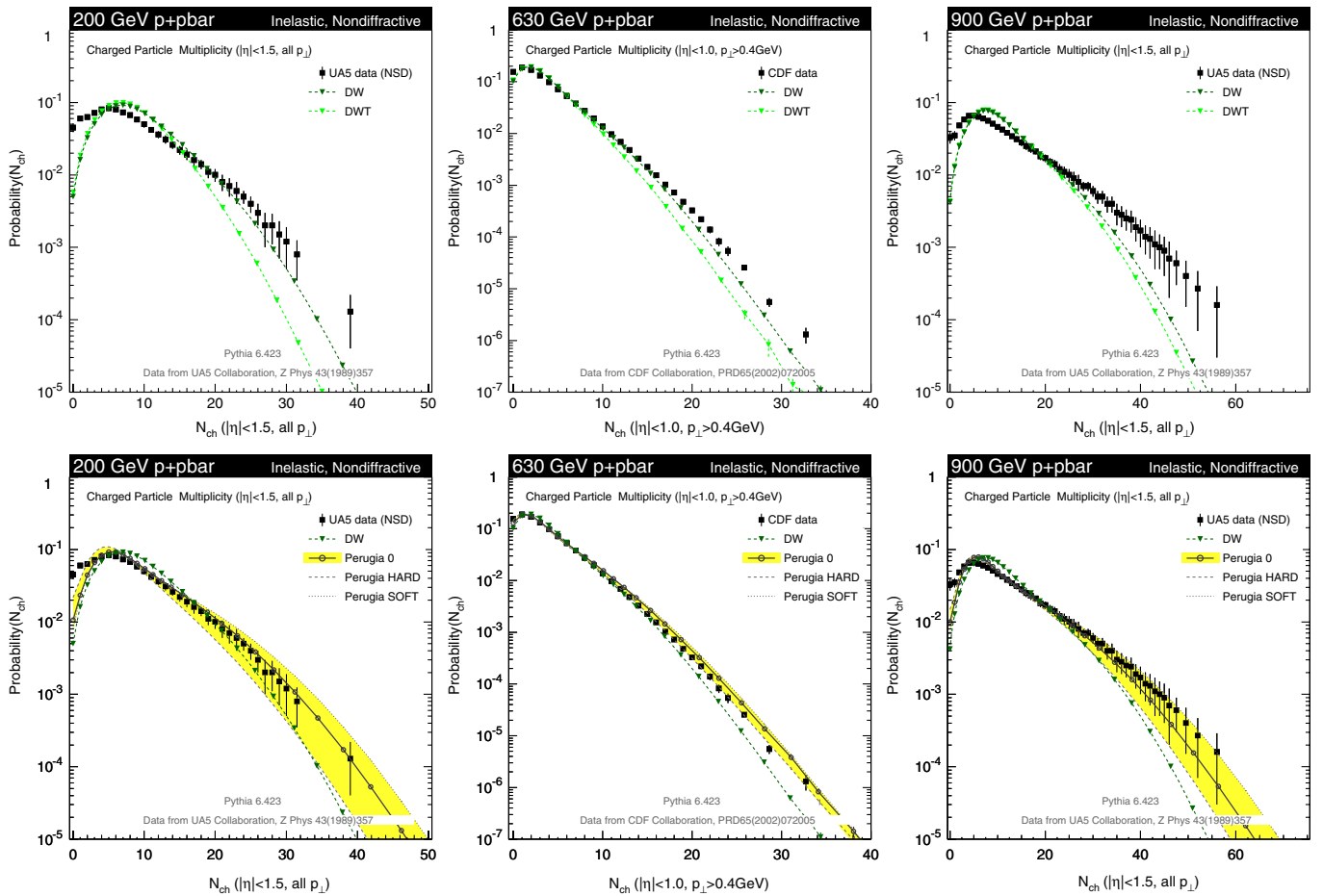


FIG. 9 (color online). Comparisons to UA5 and CDF measurements of the charged track multiplicity in minimum-bias  $p\bar{p}$  collisions at 200 GeV (left panels), 630 GeV (middle panels), and 900 GeV (right panels). Top row: Field's tunes DW and DWT. Bottom row: the main Perugia variations compared to DW. See [43] for other tunes and collider energies.

sets. In view of these tensions, we strongly recommend future studies to include comparisons at different energies.

One issue that can be clearly separated out in this discussion, however, is that the average multiplicity is sensitive to “contamination” from events of diffractive origin, while the high-multiplicity tail is not, and hence a different scaling behavior with energy (or just a different relative fraction?) of diffractive vs nondiffractive events may well generate differences between the scaling behavior of each individual moment of the multiplicity distribution. Attempting to pin down the scaling behavior moment by moment would therefore also be an interesting possible study. Since the PYTHIA 6 modeling of diffraction is relatively crude, however, we did not attempt to pursue this question further in the present study, but note that a discussion of whether these tendencies could be given other meaningful physical interpretations, e.g., in terms of low- $x$ , saturation, and/or unitarization effects, would be interesting to follow up on.

It should be safe to conclude, however, that there is clearly a need for more systematic examinations of the energy scaling behavior, both theoretically and experimentally, for both diffractive and nondiffractively enhanced event topologies separately. It would also be interesting, for instance, to attempt to separately determine the scaling behaviors for low-activity/peripheral events and for active/central events, e.g., by considering the scaling of the various moments of the multiplicity distribution and by other observables weighted by powers of the event multiplicity.

#### IV. TUNE-BY-TUNE DESCRIPTIONS

The starting point for all the Perugia tunes, apart from Perugia NOCR, was S0A-Pro, i.e., the original tune S0 [12,13,33,34], with the Tune A energy scaling (S0A), revamped to include the Professor tuning of flavor and fragmentation parameters to LEP data [29,44] (S0A-Pro). The starting point for Perugia NOCR was NOCR-Pro. From these starting points, the main hadron collider parameters were retuned to better describe the data sets described above.

As in previous versions, each tune is associated with a 3-digit number which can be given in MSTP(5) as a convenient shortcut. A complete overview of the Perugia tune parameters is given in Appendix A and a list of all the predefined tunes that are included with PYTHIA version 6.423 can be found in Appendix B.

(a) *Perugia 0 (320)*: Uses CTEQ5L parton distributions [98] (the default in PYTHIA and the most recent set available in the standalone version—see below for Perugia variations using external CTEQ6L1 and MRST LO\* distributions). Uses  $\Lambda_{\text{CMW}}$  [79] instead of  $\Lambda_{\overline{\text{MS}}}$ , which results in near-perfect agreement with the Drell-Yan  $p_{\perp}$  spectrum, both in the tail and in the peak,

cf. Figure 1. Also has slightly less color reconnections than S0(A), especially among high- $p_{\perp}$  string pieces, which improves the agreement both with the  $\langle p_{\perp} \rangle (N_{\text{ch}})$  distribution and with the high- $p_{\perp}$  tail of charged particle  $p_{\perp}$  spectra; cf. [43],  $dN/dpT$  (tail). Slightly more beam-remnant breakup than S0(A) (more baryon number transport), mostly in order to explore this possibility than due to any necessity of tuning at this point. Without further changes, these modifications would lead to a greatly increased average multiplicity as well as larger multiplicity fluctuations. To keep the total multiplicity unchanged, relative to S0A-Pro, the changes above were accompanied by an increase in the MPI infrared cutoff,  $p_{\perp 0}$ , which decreases the overall MPI-associated activity, and by a slightly smoother proton mass profile, which decreases the fluctuations. Finally, the energy scaling is closer to that of Tune A (and S0A) than to the old default scaling that was used for S0.

(b) *Perugia HARD (321)*: A variant of Perugia 0 which has a higher amount of activity from perturbative physics and counterbalances partly by having less particle production from nonperturbative sources. Thus, the  $\Lambda_{\text{CMW}}$  value is used for ISR, together with a renormalization scale for ISR of  $\mu_R = \frac{1}{2} p_{\perp}$ , yielding a comparatively hard Drell-Yan  $p_{\perp}$  spectrum; cf. the dashed curve labeled HARD in the right pane of Fig. 1. It also has a slightly larger phase space for both ISR and FSR, uses higher-than-nominal values for FSR, and has a slightly harder hadronization. To partly counterbalance these choices, it has less primordial  $k_T$ , a higher IR cutoff for the MPI, and more active color reconnections, yielding a comparatively high curve for  $\langle p_{\perp} \rangle (N_{\text{ch}})$ ; cf. Fig. 5. Warning: this tune has more ISR but also more FSR. The final number of reconstructed jets may therefore not appear to change very much, and if the number of ISR jets is held fixed (e.g., by matching), this tune may even produce *fewer* events, due to the increased broadening. For a full ISR/FSR systematics study, the amount of ISR and FSR should be changed independently.

(c) *Perugia SOFT (322)*: A variant of Perugia 0 which has a lower amount of activity from perturbative physics and makes up for it partly by adding more particle production from nonperturbative sources. Thus, the  $\Lambda_{\overline{\text{MS}}}$  value is used for ISR, together with a renormalization scale of  $\mu_R = \sqrt{2} p_{\perp}$ , yielding a comparatively soft Drell-Yan  $p_{\perp}$  spectrum; cf. the dotted curve labeled SOFT in the right pane of Fig. 1. It also has a slightly smaller phase space for both ISR and FSR, uses lower-than-nominal values for FSR, and has a slightly softer hadronization. To partly counterbalance these choices, it has a more sharply peaked proton mass distribution, a more active beam-remnant fragmentation, a slightly lower IR cutoff for the MPI, and slightly less active color reconnections, yielding a comparatively low curve for  $\langle p_{\perp} \rangle (N_{\text{ch}})$ ; cf. Fig. 5. Again, a more complete variation would be to vary the amount of ISR and FSR independently, at the price of introducing two



more variations (see above). We encourage users that desire a complete ISR/FSR systematics study to make these additional variations on their own.

(d) *Perugia 3 (323)*: A variant of Perugia 0 which has a different balance between MPI and ISR and a different energy scaling. Instead of a smooth dampening of ISR all the way to zero  $p_{\perp}$ , this tune uses a sharp cutoff at 1.25 GeV, which produces a slightly harder ISR spectrum. The additional ISR activity is counterbalanced by a higher infrared MPI cutoff. Since the ISR cutoff is independent of the collider c.m. energy in this tune, the multiplicity would nominally evolve very rapidly with energy. To offset this, the MPI cutoff itself must scale very quickly; hence this tune has a very large value of the scaling power of that cutoff. This leads to an interesting systematic difference in the scaling behavior, with ISR becoming an increasingly more important source of particle production as the energy increases in this tune, relative to Perugia 0. This is illustrated in Fig. 10, where we show the scaling of the min-bias

charged multiplicity distribution and the Drell-Yan  $p_{\perp}$  spectrum between the Tevatron (left panel) and the LHC at 14 TeV (right panel). One sees that, while the overall multiplicity grows less fast with energy in Perugia 3, the position of the soft peak in Drell-Yan becomes harder, reflecting the relative increase in ISR, despite the decrease in MPI.

(e) *Perugia NOCR (324)*: An update of NOCR-Pro that attempts to fit the data sets as well as possible, without invoking any explicit color reconnections. Can reach an acceptable agreement with most distributions, except for the  $\langle p_{\perp} \rangle(N_{\text{ch}})$  one; cf. Fig. 5. Since there is a large amount of “color disturbance” in the remnant, this tune gives rise to a very large amount of baryon number transport, even greater than for the SOFT variant above.

(f) *Perugia X (325)*: A variant of Perugia 0 which uses the MRST LO\* PDF set [82]. Because of the increased gluon densities, a slightly lower ISR renormalization scale and a higher MPI cutoff than for Perugia 0 is used. Note

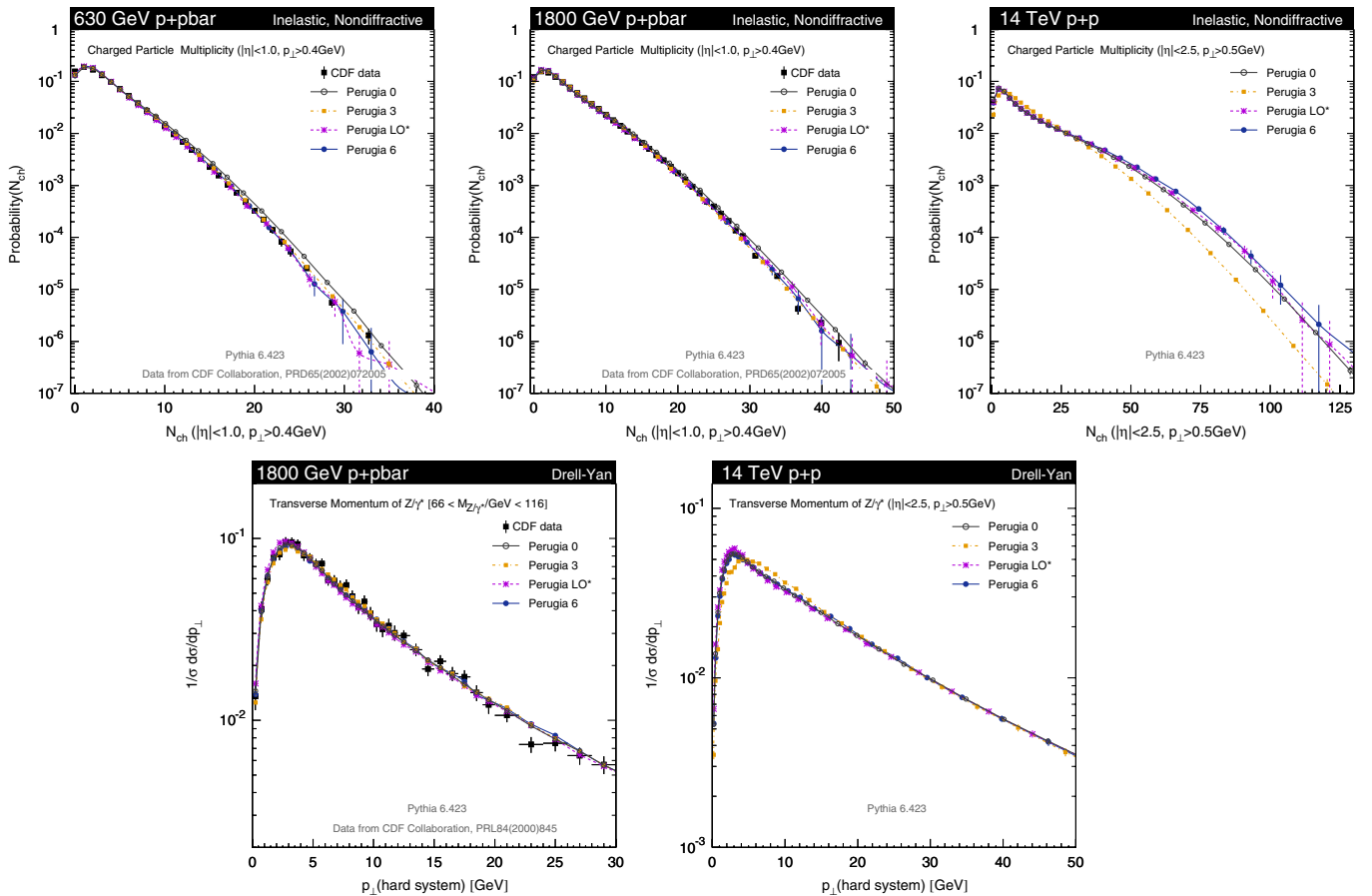


FIG. 10 (color online). Charged particle multiplicity and Drell-Yan  $p_{\perp}$  spectra at the Tevatron (left and middle) and at the LHC at 14 TeV (right) for the Perugia 0, 3, LO\*, and 6 tunes. In particular, the Perugia 3 curve on the lower right-hand plot illustrates the consequences of choosing a different regularization procedure for ISR in the infrared, which shifts the position of the infrared peak of the Drell-Yan  $p_{\perp}$  spectrum without affecting the tail of the distribution.

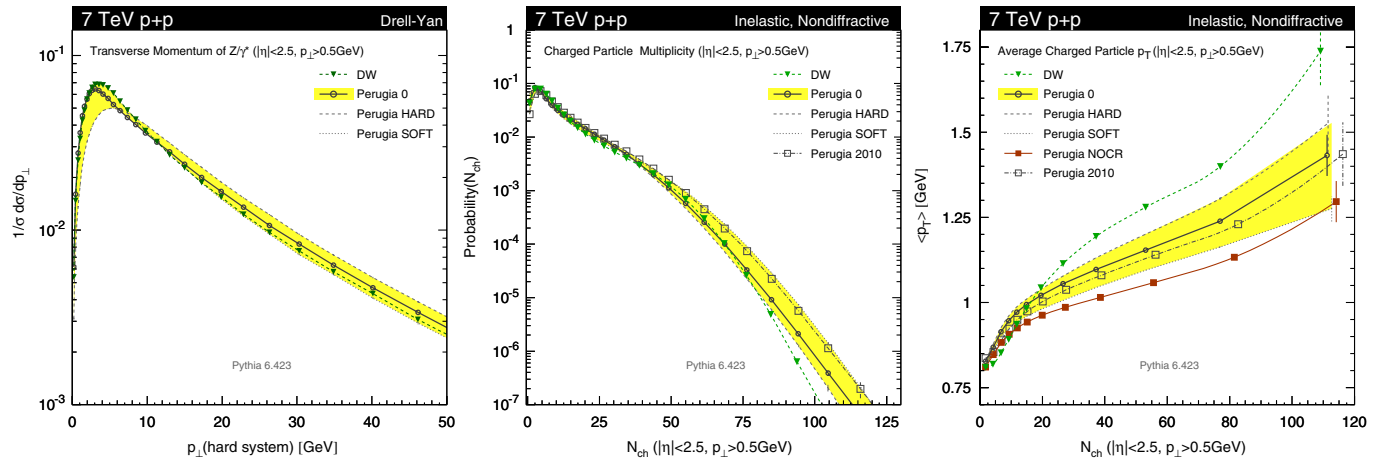


FIG. 11 (color online). Perugia predictions for the  $p_{\perp}$  of Drell-Yan pairs (left panel), the charged track multiplicity in min-bias (center panel), and the average track  $p_{\perp}$  vs  $N_{\text{ch}}$  in min-bias (right panel) at the LHC at 7 TeV. See [43] for other tunes and collider energies.

that, since we are not yet sure the implications of using LO\* for the MPI interactions have been fully understood, this tune should be considered experimental for the time being. In Fig. 10, we see that the choice of PDF does not greatly affect either the min-bias multiplicity or the Drell-Yan  $p_{\perp}$  distribution, once the slight retuning has been done. Thus, this tune is not intended to differ significantly from Perugia 0, but only to allow people to explore the LO\* set of PDFs without ruining the tuning. See [43], Perugia PDFs for more distributions.

(g) *Perugia 6 (326)*: A variant of Perugia 0 which uses the CTEQ6L1 PDF set [99]. Identical to Perugia 0 in all other respects, except for a slightly lower MPI infrared cutoff at the Tevatron and a lower scaling power of the MPI infrared cutoff (in other words, the CTEQ6L1 distributions are slightly lower than the CTEQ5L ones, on average, and hence a lower regularization scale can be tolerated). The predictions obtained are similar to those of Perugia 0; cf., e.g., Fig. 10 and [43].

(h) *Perugia 2010 (327)*: A variant of Perugia 0 with the amount of FSR outside resonance decays increased to agree with the level inside them (specifically the Perugia-0 value for hadronic Z decays at LEP is used for FSR also outside Z decays in Perugia 2010, where Perugia 0 uses the lower  $\alpha_s$  value derived from the PDFs instead), in an attempt to bracket the description of hadronic event shapes relative to the comparison of Perugia 0 to NLO + NLL resummations in [50] and also to improve the description of jet shapes [49]. The total strangeness yield has also been increased, since the original parameters, tuned by Professor, were obtained for the  $Q^2$ -ordered shower and small changes were observed when going to the  $p_{\perp}$ -ordered ones. High- $z$  fragmentation has been modified by a slightly larger infrared cutoff, which hardens the fragmentation spectrum slightly. The amount of baryon

number transport has been increased slightly, mostly in order to explore the consequences of the junction fragmentation framework better,<sup>7</sup> and the color reconnection model has been changed to the newest one, MSTP(95) = 8. See [43] for plots using this tune.

(i) *Perugia K (328)*: A variant of Perugia 2010 that introduces a  $K$  factor on the QCD  $2 \rightarrow 2$  scattering cross sections used in the multiple-parton-interaction framework. The  $K$  factor applied is set to a constant value of 1.5. This should make the underlying event more “jetty” and pushes the underlying-event activity toward higher  $p_{\perp}$ . To compensate for the increased activity at higher  $p_{\perp}$ , the infrared regularization scale is larger for this tune; cf. Table IV in Appendix A. It does not give an extremely good central fit to all data, but represents a theoretically interesting variation to explore.

## V. EXTRAPOLATION TO THE LHC

### A. “Predictions”

Part of the motivation for updating the S0 family of tunes was specifically to improve the constraints on the energy scaling to come up with tunes that extrapolate more reliably to the LHC. This is not to say that the uncertainty is still not large, but as mentioned above, it does seem that, e.g., the default PYTHIA scaling is not able to account for the scaling between the lower-energy data sets, and so this is naturally reflected in the updated parameters.

<sup>7</sup>Although there is room in the model to increase the baryon asymmetry further, this would also increase the frequency of multi-junction-junction strings in  $p\bar{p}$  events, which PYTHIA 6 is currently not equipped to deal with, and hence the strength of this effect was left at an intermediate level [cf. PARP(8) in Table IV in Appendix A].

TABLE I. Best-guess predictions for the mean density of charged tracks for min-bias  $pp$  collisions at several different LHC energies. These numbers should be compared to data corrected to 100% track finding efficiency for tracks with  $|\eta| < 2.5$  and  $p_{\perp} > 0.5$  GeV and 0% efficiency outside that region. The definition of a stable particle was set at  $c\tau \geq 10$  mm (e.g., the two tracks from a  $\Lambda^0 \rightarrow p^+ \pi^-$  decay were not counted). The  $\pm$  values represent the estimated uncertainty, based on the Perugia tunes. No simulation of diffraction was included in these numbers.

	Predictions for mean densities of charged tracks (inelastic, nondiffractive events)				
	$\frac{\langle N_{\text{ch}} \rangle_{N_{\text{ch}} \geq 0}}{\Delta\eta\Delta\phi}$	$\frac{\langle N_{\text{ch}} \rangle_{N_{\text{ch}} \geq 1}}{\Delta\eta\Delta\phi}$	$\frac{\langle N_{\text{ch}} \rangle_{N_{\text{ch}} \geq 2}}{\Delta\eta\Delta\phi}$	$\frac{\langle N_{\text{ch}} \rangle_{N_{\text{ch}} \geq 3}}{\Delta\eta\Delta\phi}$	$\frac{\langle N_{\text{ch}} \rangle_{N_{\text{ch}} \geq 4}}{\Delta\eta\Delta\phi}$
LHC 0.9 TeV	$0.21 \pm 0.03$	$0.22 \pm 0.03$	$0.24 \pm 0.02$	$0.26 \pm 0.02$	$0.30 \pm 0.02$
LHC 2.36 TeV	$0.27 \pm 0.03$	$0.28 \pm 0.03$	$0.30 \pm 0.02$	$0.33 \pm 0.02$	$0.36 \pm 0.02$
LHC 7 TeV	$0.36 \pm 0.04$	$0.37 \pm 0.04$	$0.39 \pm 0.04$	$0.42 \pm 0.05$	$0.46 \pm 0.04$
LHC 10 TeV	$0.40 \pm 0.05$	$0.41 \pm 0.05$	$0.43 \pm 0.05$	$0.46 \pm 0.06$	$0.50 \pm 0.06$
LHC 14 TeV	$0.44 \pm 0.06$	$0.45 \pm 0.06$	$0.47 \pm 0.06$	$0.51 \pm 0.06$	$0.54 \pm 0.07$

In Fig. 11, we compare the main Perugia variations to Field's Tune DW on the Drell-Yan  $p_{\perp}$  distribution (using the CDF cuts), the charged track multiplicity distribution in (inelastic, nondiffractive) minimum-bias collisions, and the average track  $p_{\perp}$  as a function of multiplicity at the initial LHC center-of-mass energy of 7 TeV. We hope this helps to give a feeling for the kind of ranges spanned by the Perugia tunes (the PDF variations give almost identical results to Perugia 0 for these distributions and are not shown). The Perugia 2010 variation gives the same Drell-Yan  $p_{\perp}$  spectrum and is therefore not shown in the left-hand pane). A full set of plots including also the 14 TeV center-of-mass energy, for both the central region,  $|\eta| < 2.5$ , and the region  $1.8 < \eta < 4.9$  covered by LHCb, can be found on the Web [43].

However, in addition to these plots, we thought it would be interesting to make at least one set of numerical predictions for an infrared sensitive quantity that could be

tested with the very earliest high-energy LHC data. We therefore used the Perugia variations to get an estimate for the mean multiplicity of charged tracks in (inelastic, nondiffractive) minimum-bias  $pp$  collisions at center-of-mass energies of 0.9, 2.36, 7, 10, and 14 TeV, as shown in Table I. In order to facilitate comparison with data sets that may include diffraction in the first few multiplicity bins, we recomputed the means with up to the first 4 bins excluded, and model uncertainties were inflated slightly for the first two bins. The uncertainty estimates correspond to roughly twice the largest difference between individual models and only drop below 10% near the collider energies used to constrain the models and then only when the lowest-multiplicity bins are excluded. Note also, however, that the uncertainties nowhere become larger than 20%. This presumably still underestimates the full theoretical uncertainty, due to intrinsic limitations in our ability to vary the models, but we hope nonetheless that it furnishes a useful first estimate.

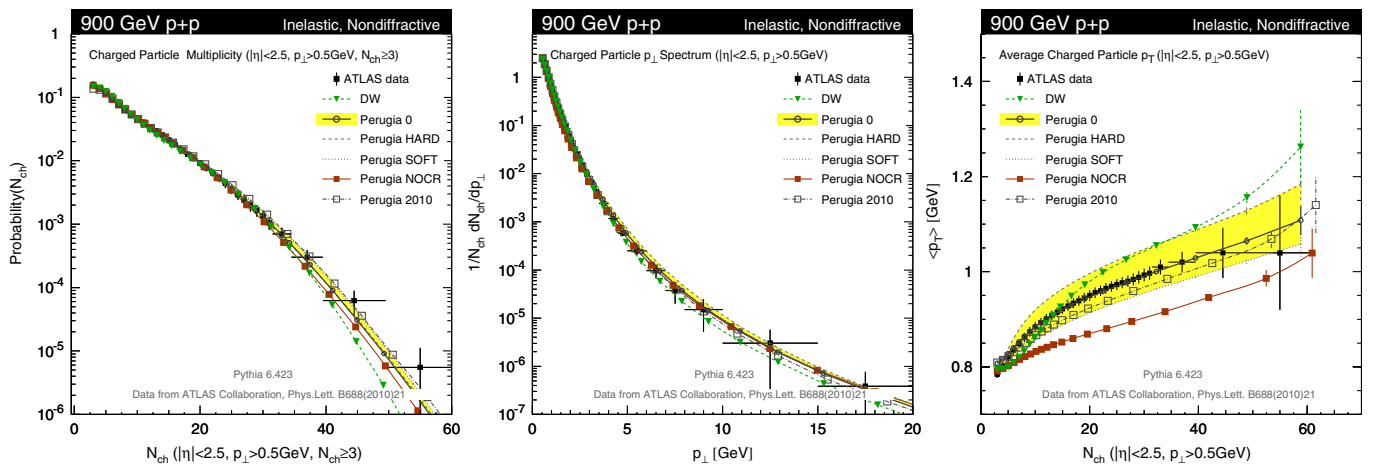


FIG. 12 (color online). Perugia predictions for the charged multiplicity (left panel),  $p_{\perp}$  (center panel), and  $\langle p_{\perp} \rangle(N_{\text{ch}})$  (right panel) distributions in inelastic, nondiffractive  $pp$  collisions at 900 GeV, compared with ATLAS data. See [43] for other tunes and collider energies.

### B. Comparison to the current LHC data

At a late stage while preparing this article, data from the initial LHC runs at 900 GeV became available in the HepDATA Web repository. We were therefore able to include a comparison of Perugia 0 and a few main variations to the 900 GeV ATLAS data [63]. We here explicitly omit bins with  $N_{\text{ch}} < 3$  in the multiplicity and  $\langle p_{\perp} \rangle(N_{\text{ch}})$  distributions since we did not include diffractive events in the simulation. The resulting comparisons are shown in Fig. 12.

The overall agreement between the models and the data is good, which is not surprising given that the 900 GeV beam energy lies well within the energy span inside which the models were tuned. One point that may be worth remarking on is that the models appear to be undershooting the tail of the multiplicity distribution slightly (left panel). This confirms the tendency already observed in the comparison to the UA5 data, cf. Fig. 9 while the models had a tendency to overshoot the tails of the Tevatron distributions, cf. Figs. 3 and 9. Combined with early indications at 7 TeV from ALICE [100] and CMS [101] that, likewise, confirm an undershooting by the models of the high-multiplicity tail, we observe that it may be particularly difficult to describe both the Tevatron and LHC data sets simultaneously and that more work in this direction would be fruitful. One way of getting closer to an apples-to-apples comparison in a study of this particular issue would be to perform an LHC measurement applying the same cuts as those used by the CDF min-bias analysis.

## VI. CONCLUSIONS

We have presented a set of updated parameter sets (tunes) for the interleaved  $p_{\perp}$ -ordered shower and underlying-event model in PYTHIA 6.4. These parameter sets include the revisions to the fragmentation and flavor parameters obtained by the Professor group [29,44]. The new sets further include more Tevatron data and more data from different collider c.m. energies in an attempt to simultaneously improve the overall description of the Tevatron data while also improving the reliability of the extrapolations to the LHC. We have also attempted to deliver a first set of “theoretical uncertainty bands,” by including alternative tunes with systematically different parameter choices. The new tunes are available from PYTHIA version 6.4.23, via the routine PYTUNE or, alternatively, via the switch MSTP(5).

Our conclusions are that reasonably good overall fits can be obtained, at the 10%–20% level, but that the contribution of diffractive processes and the scaling of the overall activity with collider energy are still highly uncertain. Other interesting questions to pursue concern the spectrum of ultrahard single hadrons with momenta above 30 GeV [57,90–93], the (possibly connected)

question of collective effects in  $pp$ , and the dynamics driving such effects, the contribution and properties of diffractive interactions, tests of jet universality by constraining fragmentation models better *in situ* at hadron colliders as compared to constraints coming from LEP and HERA, and the question of the relative balance between different particle production mechanisms with different characteristics, e.g., between soft beam-remnant fragmentation, multiple parton interactions, and traditional parton-shower/radiative corrections to the fundamental scattering processes.

We note that these tunes still only included LEP, Drell-Yan, and minimum-bias data directly, and that the lowest-multiplicity bins of the latter were ignored due to their relatively stronger sensitivity to diffractive physics which we deemed beyond the scope of this analysis to attack. Furthermore, only one Drell-Yan distribution was used, the inclusive  $p_{\perp}$  spectrum. Leading-jet,  $V/\gamma + \text{jet}(s)$ , underlying-event, and jet structure observables were not considered explicitly. We wish to emphasize that such studies furnish additional important inputs both to tuning and to jet calibration efforts through such observables as jet rates, jet pedestals, jet masses, jet-jet masses (and interjet distances), jet profiles, and dedicated jet substructure variables.

We hope these tunes will be useful to the RHIC, Tevatron, and LHC communities.

## ACKNOWLEDGMENTS

The Perugia tunes derive their names from the Perugia MPI Workshop in 2008, which brought people from different communities together, and helped us take some steps toward finding a common language. We thank the Fermilab computing division, S. Timm, in particular, and the Fermilab theory group for providing and maintaining excellent dedicated computing resources without which the large runs necessary for this tuning effort would have been impossible. We acknowledge many fruitful interactions with the RHIC, Tevatron, and LHC experimental communities, and are particularly grateful to B. Cooper, L. Galtieri, B. Heinemann, G. Hesketh, D. Kar, P. Lenzi, A. Messina, and L. Tomkins for detailed counterchecks and feedback. This work was supported in part by the Marie Curie research training network “MCnet” (Contract No. MRTN-CT-2006-035606) and by the U.S. Department of Energy under Contract No. DE-AC02-07CH11359.

## APPENDIX A: PARAMETERS FOR THE PERUGIA TUNES

Tables II, III, and IV give an overview of the parameter settings in PYTHIA corresponding to the Perugia tunes described in this paper. The settings for the previous “best” tune of the  $p_{\perp}$ -ordered model, Tune S0A-Pro, are included for reference.

TABLE II. Final-state radiation and hadronization parameters of the Perugia tunes compared to S0A-Pro. For more information on each parameter, see [14].

Parameter	Type	S0A <sub>Pro</sub>	$P_0$	$P_{\text{HARD}}$	$P_{\text{SOFT}}$	$P_3$	$P_{\text{NOCR}}$	$P_{\text{LO}^*}$	$P_6$	$P_{2010}$	$P_K$
MSTP(5)	TUNE	310	320	321	322	323	324	325	326	327	328
PARJ(81)	FSR	0.257	0.257	0.3	0.2	0.257	0.257	0.257	0.257	0.26	0.26
PARJ(82)	FSR	0.8	0.8	0.8	0.8	0.8	0.8	0.8	0.8	1.0	1.0
MSTJ(11)	HAD	5	5	5	5	5	5	5	5	5	5
PARJ(1)	HAD	0.073	0.073	0.073	0.073	0.073	0.073	0.073	0.073	0.08	0.08
PARJ(2)	HAD	0.2	0.2	0.2	0.2	0.2	0.2	0.2	0.2	0.21	0.21
PARJ(3)	HAD	0.94	0.94	0.94	0.94	0.94	0.94	0.94	0.94	0.94	0.94
PARJ(4)	HAD	0.032	0.032	0.032	0.032	0.032	0.032	0.032	0.032	0.04	0.04
PARJ(11)	HAD	0.31	0.31	0.31	0.31	0.31	0.31	0.31	0.31	0.35	0.35
PARJ(12)	HAD	0.4	0.4	0.4	0.4	0.4	0.4	0.4	0.4	0.35	0.35
PARJ(13)	HAD	0.54	0.54	0.54	0.54	0.54	0.54	0.54	0.54	0.54	0.54
PARJ(21)	HAD	0.313	0.313	0.34	0.28	0.313	0.313	0.313	0.313	0.36	0.36
PARJ(25)	HAD	0.63	0.63	0.63	0.63	0.63	0.63	0.63	0.63	0.63	0.63
PARJ(26)	HAD	0.12	0.12	0.12	0.12	0.12	0.12	0.12	0.12	0.12	0.12
PARJ(41)	HAD	0.49	0.49	0.49	0.49	0.49	0.49	0.49	0.49	0.35	0.35
PARJ(42)	HAD	1.2	1.2	1.2	1.2	1.2	1.2	1.2	1.2	0.9	0.9
PARJ(46)	HAD	1.0	1.0	1.0	1.0	1.0	1.0	1.0	1.0	1.0	1.0
PARJ(47)	HAD	1.0	1.0	1.0	1.0	1.0	1.0	1.0	1.0	1.0	1.0

TABLE III. Parton-density, initial-state radiation, and primordial  $k_T$  parameters of the Perugia tunes compared to S0A-Pro. For more information on each parameter, see [14].

Parameter	Type	S0A <sub>Pro</sub>	$P_0$	$P_{\text{HARD}}$	$P_{\text{SOFT}}$	$P_3$	$P_{\text{NOCR}}$	$P_{\text{LO}^*}$	$P_6$	$P_{2010}$	$P_K$
MSTP(5)	TUNE	310	320	321	322	323	324	325	326	327	328
MSTP(51)	PDF	7	7	7	7	7	7	20650	10042	7	7
MSTP(52)	PDF	1	1	1	1	1	1	2	2	1	1
MSTP(3)		2	2	2	2	2	2	2	2	1	1
MSTU(112)										4	4
PARU(112)										0.192	0.192
PARP(1)	ME									0.192	0.192
PARP(61)	ISR									0.192	0.192
PARP(72)	IFSR									0.26	0.26
MSTP(64)	ISR	2	3	3	2	3	3	3	3	3	3
PARP(64)	ISR	1.0	1.0	0.25	2.0	1.0	1.0	2.0	1.0	1.0	1.0
MSTP(67)	ISR	2	2	2	2	2	2	2	2	2	2
PARP(67)	ISR	4.0	1.0	4.0	0.25	1.0	1.0	1.0	1.0	1.0	1.0
PARP(71)	IFSR	4.0	2.0	4.0	1.0	2.0	2.0	2.0	2.0	2.0	2.0
MSTP(70)	ISR	2	2	0	1	0	2	2	2	2	2
PARP(62)	ISR			1.25		1.25					
PARP(81)	ISR				1.5						
MSTP(72)	ISR	0	1	1	0	2	1	1	1	2	2
MSTP(91)	BR	1	1	1	1	1	1	1	1	1	1
PARP(91)	BR	2.0	2.0	1.0	2.0	1.5	2.0	2.0	2.0	2.0	2.0
PARP(93)	BR	10.0	10.0	10.0	10.0	10.0	10.0	10.0	10.0	10.0	10.0

TABLE IV. Underlying-event, beam-remnant, and color-reconnection parameters of the Perugia tunes compared to SOA-Pro. For more information on each parameter, see [14].

Parameter	Type	SOA <sub>Pro</sub>	$P_0$	$P_{\text{HARD}}$	$P_{\text{SOFT}}$	$P_3$	$P_{\text{NOCR}}$	$P_{\text{LO}^*}$	$P_6$	$P_{2010}$	$P_K$
MSTP(5)	TUNE	310	320	321	322	323	324	325	326	327	328
MSTP(81)	UE	21	21	21	21	21	21	21	21	21	21
PARP(82)	UE	1.85	2.0	2.3	1.9	2.2	1.95	2.2	1.95	2.05	2.45
PARP(89)	UE	1800	1800	1800	1800	1800	1800	1800	1800	1800	1800
PARP(90)	UE	0.25	0.26	0.30	0.24	0.32	0.24	0.23	0.22	0.26	0.26
MSTP(82)	UE	5	5	5	5	5	5	5	5	5	5
PARP(83)	UE	1.6	1.7	1.7	1.5	1.7	1.8	1.7	1.7	1.5	1.5
PARP(84)	UE										
MSTP(33)	“K”	0	0	0	0	0	0	0	0	0	10
PARP(32)	“K”										1.5
MSTP(88)	BR	0	0	0	0	0	0	0	0	0	0
PARP(79)	BR	2.0	2.0	2.0	2.0	2.0	2.0	2.0	2.0	2.0	2.0
MSTP(89)	BR	1	1	1	0	1	2	1	1	0	0
PARP(80)	BR	0.01	0.05	0.01	0.05	0.03	0.01	0.05	0.05	0.1	0.1
MSTP(95)	CR	6	6	6	6	6	6	6	6	8	8
PARP(78)	CR	0.2	0.33	0.37	0.15	0.35	0.0	0.33	0.33	0.035	0.033
PARP(77)	CR	0.0	0.9	0.4	0.5	0.6	0.0	0.9	0.9	1.0	1.0

**APPENDIX B: OVERVIEW OF TUNES INCLUDED IN PYTHIA**

Tables V, VI, and VII give an overview of the tune presets that have so far been implemented in PYTHIA, as

of version 6.4.23. They can be obtained either by setting MSTP(5) = NNN, where NNN is the tune number, or by calling PYTUNE(NNN) before the call to PYINIT. It is not advisable to do both. Note that, when MSTP(5) is used,

TABLE V. 100+:  $Q^2$ -ordered shower and “old” underlying-event model.

MSTP(5) Name	Description	Date
1st generation: Field’s CDF tunes and a few more		
100 A	: Field’s CDF Tune A	(Oct. 2002)
101 AW	: Field’s CDF Tune AW	(Apr. 2006)
102 BW	: Field’s CDF Tune BW	(Apr. 2006)
103 DW	: Field’s CDF Tune DW	(Apr. 2006)
104 DWT	: As DW but with the old default ECM scaling	(Apr. 2006)
105 QW	: Field’s CDF Tune QW using CTEQ6.1M	
106 ATLAS-DC2	: Moraes’ (old) ATLAS tune (“Rome”)	
107 ACR	: Tune A modified with new CR model	(Mar. 2007)
108 D6	: Field’s CDF Tune D6 using CTEQ6L1	
109 D6T	: Field’s CDF Tune D6T using CTEQ6L1	
2nd generation: The same, but with Professor’s LEP parameters		
110 A-Pro	: Tune A, but with Professor’s LEP parameters	(Oct. 2008)
111 AW-Pro	: Tune AW, but with Professor’s LEP parameters	(Oct. 2008)
112 BW-Pro	: Tune BW, but with Professor’s LEP parameters	(Oct. 2008)
113 DW-Pro	: Tune DW, but with Professor’s LEP parameters	(Oct. 2008)
114 DWT-Pro	: Tune DWT, but with Professor’s LEP parameters	(Oct. 2008)
115 QW-Pro	: Tune QW, but with Professor’s LEP parameters	(Oct. 2008)
116 ATLAS-DC2-Pro	: ATLAS-DC2/Rome, but with Professor’s LEP parameters	(Oct. 2008)
117 ACR-Pro	: Tune ACR, but with Professor’s LEP parameters	(Oct. 2008)
118 D6-Pro	: Tune D6, but with Professor’s LEP parameters	(Oct. 2008)
119 D6T-Pro	: Tune D6T, but with Professor’s LEP parameters	(Oct. 2008)
3rd generation: Complete $Q^2$ -ordered tune by Professor		
129 Pro-Q2O	: Professor $Q^2$ -ordered tune	(Feb. 2009)

TABLE VI. 200+: Intermediate and hybrid models.

MSTP(5) Name	Description	Date
200 IM 1	: Intermediate model: new UE, Q2-ord. showers, new CR	
201 APT	: Tune A w. $pT$ -ordered FSR	(Mar. 2007)
211 APT-Pro	: Tune APT, with LEP tune from Professor	(Oct. 2008)
221 Perugia APT	: Perugia update of APT-Pro	(Feb. 2009)
226 Perugia APT6	: Perugia update of APT-Pro w. CTEQ6L1	(Feb. 2009)

TABLE VII. 300+:  $p_{\perp}^2$ -ordered shower and interleaved underlying-event model.

MSTP(5) Name	Description	Date
1st generation: Sandhoff-Skands CDF min-bias tunes and a few more		
300 SO	: Sandhoff-Skands tune using the S0 CR model	(Apr. 2006)
301 SI	: Sandhoff-Skands tune using the S1 CR model	(Apr. 2006)
302 S2	: Sandhoff-Skands tune using the S2 CR model	(Apr. 2006)
303 S0A	: S0 with ‘‘Tune A’’ UE energy scaling	(Apr. 2006)
304 NOCR	: ‘‘Best try’’ without CR	(Apr. 2006)
305 Old	: Original (primitive) CR model	(Aug. 2004)
306 ATLAS-CSC	: Moraes’ $p_{\perp}$ -ordered ATLAS tune w. CTEQ6L1	
2nd generation: The same, but with Professor’s LEP parameters		
310 S0-Pro	: S0, but with Professor’s LEP parameters	(Oct. 2008)
311 S1-Pro	: S1, but with Professor’s LEP parameters	(Oct. 2008)
312 S2-Pro	: S2, but with Professor’s LEP parameters	(Oct. 2008)
313 S0A-Pro	: S0A, but with Professor’s LEP parameters	(Oct. 2008)
314 NOCR-Pro	: NOCR, but with Professor’s LEP parameters	(Oct. 2008)
315 Old-Pro	: Old, but with Professor’s LEP parameters	(Oct. 2008)
3rd generation: The Perugia, Professor, and ATLAS MC09 $pT$ -ordered tunes		
320 Perugia 0	: Perugia update of S0-Pro	(Feb. 2009)
321 Perugia HARD	: More ISR, more FSR, Less MPI, less BR, less HAD	(Feb. 2009)
322 Perugia SOFT	: Less ISR, less FSR, more MPI, more BR, more HAD	(Feb. 2009)
323 Perugia 3	: Alternative to Perugia 0, with different ISR/MPI balance & different scaling to LHC & RHIC	(Feb. 2009)
324 Perugia NOCR	: Perugia update of NOCR-Pro	(Feb. 2009)
325 Perugia*	: Perugia tune w. (external) MRSTLO* PDFs	(Feb. 2009)
326 Perugia 6	: Perugia tune w. (external) CTEQ6L1 PDFs	(Feb. 2009)
327 Perugia 2010	: Perugia 0 with more FSR off ISR and more strangeness	(Mar. 2010)
328 Perugia K	: Perugia 2010 with a $K$ factor on the MPI cross sections	(Mar. 2010)
329 Pro-pT0	: Professor $pT$ -ordered tune w. S0 CR model	(Feb. 2009)
330 MC09	: ATLAS MC09 tune with (external) LO* PDFs	(2009)
335 Pro-pT*	: Professor tune with (external) LO* PDFs	(Mar. 2009)
336 Pro-pT6	: Professor tune with (external) CTEQ6L1 PDFs	(Mar. 2009)
339 Pro-pT**	: Professor tune with (external) LO** PDFs	(Mar. 2009)

PYINIT calls PYTUNE, and the tune parameters will then overwrite any previous user modifications. Also consult the output of PYTUNE which informs you about useful

references for each tune, its parameters, and a brief description of their meaning.

- [1] A. M. Snigirev, *Phys. Rev. D* **68**, 114012 (2003).
- [2] V. L. Korotkikh and A. M. Snigirev, *Phys. Lett. B* **594**, 171 (2004).
- [3] T. Akesson *et al.* (AFS Collaboration), *Z. Phys. C* **34**, 163 (1987).
- [4] C.-E. Wulz (UA1 Collaboration), in *Proceedings of the 22nd Rencontres de Moriond, Les Arcs, France, 1987* (Editions Frontieres, Gif-sur-Yvette, France, 1987).
- [5] J. Alitti *et al.* (UA2 Collaboration), *Phys. Lett. B* **268**, 145 (1991).
- [6] F. Abe *et al.* (CDF Collaboration), *Phys. Rev. D* **47**, 4857 (1993).
- [7] F. Abe *et al.* (CDF Collaboration), *Phys. Rev. Lett.* **79**, 584 (1997).
- [8] F. Abe *et al.* (CDF Collaboration), *Phys. Rev. D* **56**, 3811 (1997).
- [9] V. M. Abazov *et al.* (D0 Collaboration), *Phys. Rev. D* **67**, 052001 (2003).
- [10] V. M. Abazov *et al.* (D0 Collaboration), *Phys. Rev. D* **81**, 052012 (2010).
- [11] C. Gwenlan *et al.* (ZEUS Collaboration), *Acta Phys. Pol. B* **33**, 3123 (2002).
- [12] T. Sjöstrand and P. Z. Skands, *Eur. Phys. J. C* **39**, 129 (2005).
- [13] T. Sjöstrand and P. Z. Skands, *J. High Energy Phys.* **03** (2004) 053.
- [14] T. Sjöstrand, S. Mrenna, and P. Skands, *J. High Energy Phys.* **05** (2006) 026.
- [15] T. Sjöstrand, S. Mrenna, and P. Skands, *Comput. Phys. Commun.* **178**, 852 (2008).
- [16] R. Corke and T. Sjöstrand, *J. High Energy Phys.* **01** (2010) 035.
- [17] Y. I. Azimov, Y. L. Dokshitzer, V. A. Khoze, and S. I. Troyan, *Z. Phys. C* **27**, 65 (1985).
- [18] Z. Koba, H. B. Nielsen, and P. Olesen, *Nucl. Phys.* **B40**, 317 (1972).
- [19] J. F. Grosse-Oetringhaus and K. Reygers, *J. Phys. G* **37**, 083001 (2010).
- [20] R. Field (CDF Collaboration), *Int. J. Mod. Phys. A* **16S1A**, 250 (2001).
- [21] A. A. Affolder *et al.* (CDF Collaboration), *Phys. Rev. D* **65**, 092002 (2002).
- [22] R. D. Field (CDF Collaboration), [arXiv:hep-ph/0201192](https://arxiv.org/abs/hep-ph/0201192).
- [23] D. E. Acosta *et al.* (CDF Collaboration), *Phys. Rev. D* **70**, 072002 (2004).
- [24] R. Field (CDF Collaboration), *Acta Phys. Pol. B* **36**, 167 (2005).
- [25] D. Kar (CDF Collaboration), [arXiv:0905.2323](https://arxiv.org/abs/0905.2323).
- [26] K. Werner, *Nucl. Phys. B, Proc. Suppl.* **175–176**, 81 (2008).
- [27] W. D. Apel *et al.* (KASCADE Collaboration), *J. Phys. G* **36**, 035201 (2009).
- [28] T. Pierog and K. Werner, *Nucl. Phys. B, Proc. Suppl.* **196**, 102 (2009).
- [29] A. Buckley, H. Hoeth, H. Lacker, H. Schulz, and J. E. von Seggern, *Eur. Phys. J. C* **65**, 331 (2010).
- [30] A. Bacchetta, H. Jung, A. Knutsson, K. Kutak, and F. von Samson-Himmelstjerna, [arXiv:1001.4675](https://arxiv.org/abs/1001.4675).
- [31] W. T. Giele, D. A. Kosower, and P. Z. Skands, *Phys. Rev. D* **78**, 014026 (2008).
- [32] P. Skands, W. Giele, and D. Kosower, “Higher-Order Corrections to Timelike Jets” (unpublished).
- [33] M. Sandhoff and P. Skands, in *Proceedings of the Les Houches Workshop on Physics at TeV Colliders, Les Houches, 2005* (LAPP, Annecy, France, 2005).
- [34] P. Skands and D. Wicke, *Eur. Phys. J. C* **52**, 133 (2007).
- [35] D. Wicke and P. Z. Skands, *Nuovo Cimento Soc. Ital. Fis. B* **123**, S1 (2008).
- [36] P. Z. Skands, [arXiv:0803.0678](https://arxiv.org/abs/0803.0678).
- [37] S. Alekhin *et al.*, [arXiv:hep-ph/0601012](https://arxiv.org/abs/hep-ph/0601012).
- [38] M. G. Albrow *et al.* (TeV4LHC QCD Working Group), [arXiv:hep-ph/0610012](https://arxiv.org/abs/hep-ph/0610012).
- [39] C. Buttar *et al.*, [arXiv:0803.0678](https://arxiv.org/abs/0803.0678).
- [40] P. Bartalini *et al.*, in *Hamburg 2008, Multiparticle Dynamics (ISMD08)* (DESY, Hamburg, 2008), pp. 406–411.
- [41] T. Sjöstrand, S. Mrenna, and P. Skands, PYTHIA update notes, <http://projects.hepforge.org/pythia6/>.
- [42] P. Z. Skands, [arXiv:0905.3418](https://arxiv.org/abs/0905.3418).
- [43] P. Skands, Peter’s PYTHIA plots, see <http://home.fnal.gov/~skands/leshouches-plots/>.
- [44] A. Buckley, H. Hoeth, H. Lacker, H. Schulz, and E. von Seggern, [arXiv:0906.0075](https://arxiv.org/abs/0906.0075).
- [45] K. Ackerstaff *et al.* (OPAL Collaboration), *Eur. Phys. J. C* **7**, 369 (1999).
- [46] C. Amsler *et al.* (Particle Data Group), *Phys. Lett. B* **667**, 1 (2008).
- [47] J. Adams *et al.* (STAR Collaboration), *Phys. Lett. B* **637**, 161 (2006).
- [48] B. I. Abelev *et al.* (STAR Collaboration), *Phys. Rev. C* **75**, 064901 (2007).
- [49] D. E. Acosta *et al.* (CDF Collaboration), *Phys. Rev. D* **71**, 112002 (2005).
- [50] A. Banfi, G. P. Salam, and G. Zanderighi, *J. High Energy Phys.* **06** (2010) 038.
- [51] A. A. Affolder *et al.* (CDF Collaboration), *Phys. Rev. Lett.* **84**, 845 (2000).
- [52] V. M. Abazov *et al.* (D0 Collaboration), *Phys. Rev. Lett.* **100**, 102002 (2008).
- [53] A. Buckley *et al.*, in [arXiv:1003.1643](https://arxiv.org/abs/1003.1643).
- [54] D. E. Acosta *et al.* (CDF Collaboration), *Phys. Rev. D* **65**, 072005 (2002).
- [55] N. Moggi, M. Mussini, and F. Rimondi, CDF Public Note 9936, see <http://www-cdf.fnal.gov/physics/new/qcd/QCD.html>.
- [56] F. Abe *et al.* (CDF Collaboration), *Phys. Rev. Lett.* **61**, 1819 (1988).
- [57] T. Aaltonen *et al.* (CDF Collaboration), *Phys. Rev. D* **79**, 112005 (2009).
- [58] T. Alexopoulos *et al.*, *Phys. Lett. B* **435**, 453 (1998).
- [59] G. J. Alner *et al.* (UA5 Collaboration), *Phys. Rep.* **154**, 247 (1987).
- [60] R. E. Ansorge *et al.* (UA5 Collaboration), *Z. Phys. C* **43**, 357 (1989).
- [61] K. Aamodt *et al.* (ALICE Collaboration), *Eur. Phys. J. C* **65**, 111 (2010).
- [62] V. Khachatryan *et al.* (CMS Collaboration), *J. High Energy Phys.* **02** (2010) 041.
- [63] G. Aad *et al.* (ATLAS Collaboration), *Phys. Lett. B* **688**, 21 (2010).
- [64] R. D. Field and R. P. Feynman, *Phys. Rev. D* **15**, 2590 (1977).



- [65] R. D. Field, econf C010630, P501 (2001) [arXiv:hep-ph/0201192](#); further recent talks available from <http://www.phys.ufl.edu/~rfield/cdf/>.
- [66] A. Banfi, G. P. Salam, and G. Zanderighi, *J. High Energy Phys.* **08** (2004) 062.
- [67] V. M. Abazov *et al.* (D0 Collaboration), *Phys. Rev. Lett.* **94**, 221801 (2005).
- [68] R. Field and R. C. Group, [arXiv:hep-ph/0510198](#).
- [69] R. Field *et al.* (CDF Collaboration), *AIP Conf. Proc.* **828**, 163 (2006).
- [70] T. Aaltonen *et al.* (CDF Collaboration), *Phys. Rev. Lett.* **102**, 232002 (2009).
- [71] M. Cacciari, G. P. Salam, and S. Sapeta, *J. High Energy Phys.* **04** (2010) 065.
- [72] T. Aaltonen *et al.* (CDF Collaboration), *Phys. Rev. D* **82**, 034001 (2010).
- [73] D. Kar, Ph.D. thesis, University of Florida, 2008 [FERMILAB-THESIS-2008-54].
- [74] T. Carli, T. Gehrmann, and S. Hoeche, *Eur. Phys. J. C* **67**, 73 (2010).
- [75] ATLAS Collaboration, ATLAS Monte Carlo Tunes for MC09, ATL-PHYS-PUB-2010-002, 2010.
- [76] B. Andersson, G. Gustafson, and B. Söderberg, *Z. Phys. C* **20**, 317 (1983).
- [77] M. G. Bowler, *Z. Phys. C* **11**, 169 (1981).
- [78] Z. Nagy and D. E. Soper, *J. High Energy Phys.* **03** (2010) 097.
- [79] S. Catani, B. R. Webber, and G. Marchesini, *Nucl. Phys.* **B349**, 635 (1991).
- [80] G. Corcella *et al.*, *J. High Energy Phys.* **01** (2001) 010.
- [81] M. Bähr *et al.*, *Eur. Phys. J. C* **58**, 639 (2008).
- [82] A. Sherstnev and R. S. Thorne, *Eur. Phys. J. C* **55**, 553 (2008).
- [83] T. Kasemets, [arXiv:1002.4376](#).
- [84] M. Bengtsson and T. Sjöstrand, *Phys. Lett. B* **185**, 435 (1987).
- [85] M. Bengtsson and T. Sjöstrand, *Nucl. Phys.* **B289**, 810 (1987).
- [86] T. Plehn, D. Rainwater, and P. Z. Skands, *Phys. Lett. B* **645**, 217 (2007).
- [87] P. Z. Skands, T. Plehn, and D. Rainwater, ECONF C 0508141, ALCPG0417 (2005), [arXiv:0511306](#).
- [88] R. Corke and T. Sjöstrand, [arXiv:1003.2384](#).
- [89] J. Alwall, S. de Visscher, and F. Maltoni, *J. High Energy Phys.* **02** (2009) 017.
- [90] F. Arleo, D. d'Enterria, and A. S. Yoon, *J. High Energy Phys.* **06** (2010) 035.
- [91] S. Albino, B. A. Kniehl, and G. Kramer, *Phys. Rev. Lett.* **104**, 242001 (2010).
- [92] M. Cacciari, G. P. Salam, and M. J. Strassler, [arXiv:1003.3433](#).
- [93] A. S. Yoon, E. Wenger, and G. Roland, [arXiv:1003.5928](#).
- [94] T. Sjöstrand and M. van Zijl, *Phys. Rev. D* **36**, 2019 (1987).
- [95] M. Campanelli and J. W. Monk, [arXiv:0910.5108](#).
- [96] T. Alexopoulos *et al.* (E735 Collaboration), *Phys. Lett. B* **353**, 155 (1995).
- [97] A. Donnachie and P. V. Landshoff, *Phys. Lett. B* **296**, 227 (1992).
- [98] H. L. Lai *et al.* (CTEQ Collaboration), *Eur. Phys. J. C* **12**, 375 (2000).
- [99] J. Pumplin *et al.*, *J. High Energy Phys.* **07** (2002) 012.
- [100] K. Aamodt *et al.* (ALICE Collaboration), *Eur. Phys. J. C* **68**, 345 (2010).
- [101] V. Khachatryan *et al.* (CMS Collaboration), *Phys. Rev. Lett.* **105**, 022002 (2010).